6-2023

Design of Hybrid Inverters Using Wideband Gap Semiconductors for Microgrid Application

Luca Gacy
University of Denver

Design of Hybrid Inverters Using Wideband Gap Semiconductors for Microgrid Application

Abstract

As the world becomes more reliant on renewable energy sources such as solar and wind power, the need for high efficiency high power inverters connected to homes is more relevant than ever. Connecting these renewable energy sources (RES) coupled with an energy storage system (ESS) to the grid through a hybrid inverter, with the highest efficiency and grid stability, is quickly becoming a necessity for the near future. This thesis explores the integration of wide band gap semiconductors for the power stage in these systems, along with the analysis of hybrid inverter topologies and structures. The goal of this thesis is to help as a resource with the decision process in components and design of systems in the home energy field. A three-phase high voltage power stage and gate driver were constructed and tested under load to verify the functionality of the inverter.

Document Type

Masters Thesis

Degree Name

M.S.

First Advisor

David Wenzhong Gao

Second Advisor

Goncalo F. Martin

Third Advisor

Mohammad Matin

Keywords

Inverter, Microgrid, Power electronics

Subject Categories

Electrical and Computer Engineering | Electrical and Electronics | Engineering | Power and Energy

Design of Hybrid Inverters Using Wideband Gap Semiconductors for Microgrid Application

A Thesis

Presented to

the Faculty of the Daniel Felix Ritchie School of Engineering and Computer Science

University of Denver

In Partial Fulfillment

of the Requirements for the Degree

Master of Science

by

Luca Gacy

June 2023

Advisor: Dr. David Gao

Author: Luca Gacy
Title: Design of Hybrid Inverters Using Wideband Gap Semiconductors for Microgrid Application
Advisor: Dr. David Gao
Degree Date: June 2023

Abstract

As the world becomes more reliant on renewable energy sources such as solar and wind power, the need for high efficiency high power inverters connected to homes is more relevant than ever. Connecting these renewable energy sources (RES) coupled with an energy storage system (ESS) to the grid through a hybrid inverter, with the highest efficiency and grid stability, is quickly becoming a necessity for the near future. This thesis explores the integration of wide band gap semiconductors for the power stage in these systems, along with the analysis of hybrid inverter topologies and structures. The goal of this thesis is to help as a resource with the decision process in components and design of systems in the home energy field. A three-phase high voltage power stage and gate driver were constructed and tested under load to verify the functionality of the inverter.

Acknowledgements

I would like to show my deepest gratitude to Dr. David Gao, my advisor, for his guidance and help in my research. It would not have been possible without his mentorship and support. I would also like to thank Dr. Carsten Markgraf, Samuel Leitenmaier, and Daniel Lengerer from University of Augsburg in Germany for our collaboration during the 2021-2022 academic year on part of this thesis. Ben Schwartz was also helpful in simulating and designing a cooling system for the testbench setup. Lastly, I would like to thank all my friends and family who have been so supportive these past two years.

Table of Contents

List of Figures

Chapter One: Introduction

1.1. Background

Hybrid inverters are becoming increasingly popular for homes with photo voltaic cells and battery storage systems while being connected to the grid, allowing for energy to be efficiently and intelligently controlled. As the world shifts towards renewable energy, they are an integral part of the transition. Some of the issues with older systems are their cost, form factor, and efficiency, making them suboptimal in a competitive market. This thesis will aim to offer potential solutions using newer technology such as wide band gap semiconductors along with different inverter topologies and structures. With the increasing demand for renewable energy solutions, the adoption of hybrid inverters is set to increase as they offer a reliable, cost-effective, and sustainable way to connect DC systems to the AC grid. The use of wide band gap semiconductors in hybrid inverters requires more research and this thesis aims to add to that progress.

There are many applications of inverters. When a three-phase motor is used to power any type of machinery, an inverter is needed. This can range from electric cars, public transportation, to manufacturing equipment. They are also used when connecting DC systems to the grid energy distribution system which runs on 60hz in the US. This is required in systems like an energy storage system as in a battery or potentially an electric vehicle, or solar cells.

1.2.Motivation

These efforts not only reduce energy costs, but also decrease carbon emissions to combat climate change which is more relevant than ever. Improving technology in this area and providing resources to help the development of hybrid inverters in the future is the goal for this thesis. The recent introduction of these new wide band gap semi-conductors has lots of potential in this field and could play a role in providing homeowners with compact and highly efficient systems to make adding renewable energy to their home more economical. A potential shift to smaller microgrid communities may be coming [1] due to the benefits they provide with decentralized power. Having a system designed to operate as a network of ESS and RES is essential for this possibility to become a reality. Grid forming inverters are the system to connect all these systems together and the more efficient and affordable they are, the larger impact it will have on the planet.

1.3. Problem Statement

The goal of this thesis is to validate SiC MOSFETs as a switching method used in high performance inverters for microgrid application along with the drive train in electric vehicles. This thesis will also explore different control methods, in a simulated environment, for inverters to offer a study to aid with the development of future projects. An inverter power stage and gate driver will be developed to test and validate the use case of SiC MOSFETs, and PSIM simulations will be used to build an adaptable model that can be used to simulate various control methods.

Chapter Two: Literature Review

2.1 Inverter Overview

Inverters are used in many industries from power distribution, power generation, transportation, and others. The main purpose of inverters is to convert a direct current power source into an alternating current load. Bidirectional inverters are able to have the flow of power in either direction. This can be helpful in cases like a battery where sometimes energy is flowing into the battery and sometimes it is flowing out depending on the current state of the system.

Inverters are mostly used in power electronics and in general are controlled by a low voltage system controlling an isolated gate driver that generates the higher voltage signal that is sent to a power module which performs the high voltage switching.

Depending on the application, there are several types of inverters that can be used. The first most fundamental type is a single-phase inverter. This takes one DC voltage and generates one periodic output at the desired frequency and characteristic like what type of wave; in most cases, a wave that is as close to a perfect sinewave is preferred. There are two main types of single-phase inverters: half bridge and full bridge inverters as shown in Figure 1.

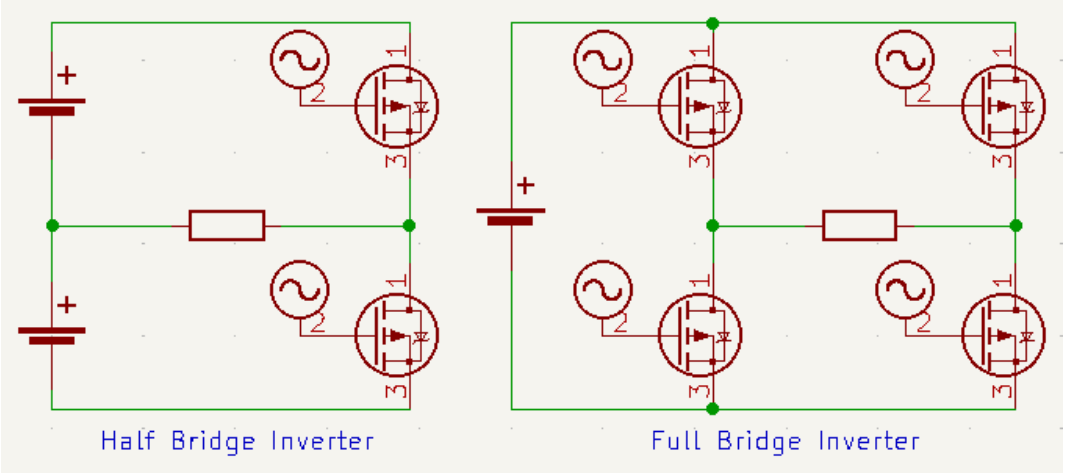

Figure 1: Half Bridge and Full Bridge Inverter Schematic

However, in many applications, a three-phase inverter is needed. This takes a DC source and generates three sinusoidal outputs that are offset by 120 degrees each. These three signals are generated by reference signals provided by a controller and modulated with a carrier frequency to generate the output.

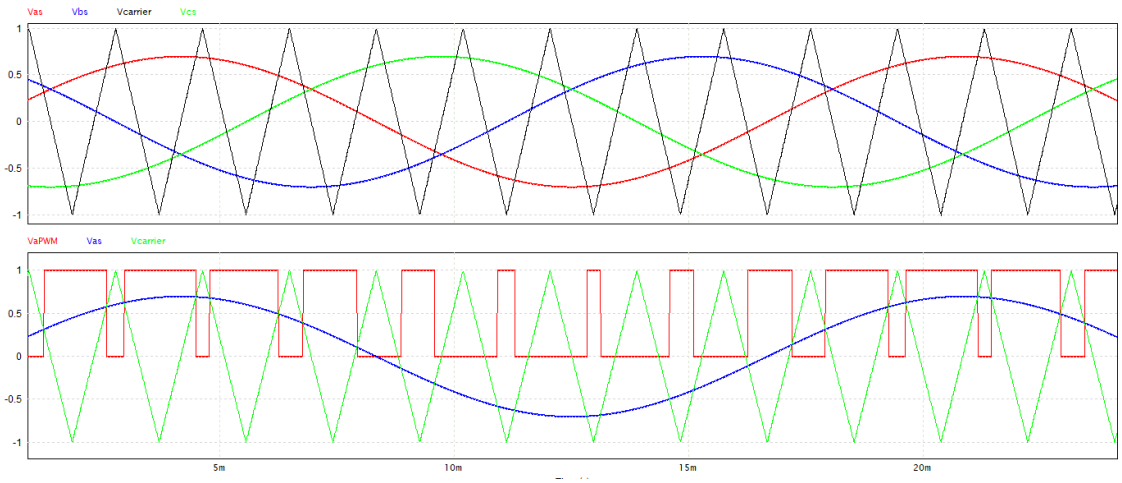

Figure 2: Three phase inverter example graph

Three phase inverters in several different topologies will be discussed in this thesis. This is due to the fact that the batteries and solar when connected to a house need to be

connected to the three-phase power distributed from the grid. The image shown in Figure 2 shows the generated output in the red, creating the PWM signal (bottom graph).

2.2. Grid Connected Power Electronics

Inverters Connecting a building to the grid can be done in several ways, all with advantages and disadvantages. These inverters are distinguished into three groups; these groups are grid forming inverters (GFM), grid following inverters (GFL), and grid supporting inverters (GS). [2]

Grid forming inverters are becoming increasingly important for microgrids due to the growing need for reliable, resilient, and efficient energy systems. Microgrids are small-scale, localized power systems that can operate independently or in conjunction with the larger electrical grid. They often include RESs such as solar panels, wind turbines, and ESSs, which can provide more sustainable and cost-effective power than traditional grid power [1].

One of the key challenges of microgrids is ensuring that they remain stable and in sync with the rest of the electrical grid. Grid forming inverters play a critical role in this regard. They are able to independently control and stabilize the voltage and frequency of the microgrid, enabling it to operate seamlessly in parallel with the main grid. [2] This is essential for maintaining a reliable and resilient power supply, as any disruptions or deviations from standard frequency and voltage levels can lead to power outages and damage to electrical equipment.

In addition to their ability to stabilize microgrids, grid forming inverters also offer several other benefits. They can enable the integration of temporal renewable energy

sources, such as solar and wind, into microgrids, providing a more sustainable and environmentally friendly power source. They can also enable microgrids to operate independently during grid outages or other emergencies, providing a reliable source of power for critical infrastructure and services. [3]

Rather than controlling the voltage amplitude and frequency directly like GFMs, grid following inverters control their real and reactive power. They often use phase locked loop synchronization to stay connected to the grid. Since they require the frequency to be provided by the grid, a network of GFLs is not a possibility invalidating them as a solution unlike GFMs. Both GFLs and grid supporting inverters are reactive to the grid, meaning they can exacerbate instabilities in the grid rather than damping them like GFMs. For this reason, GFM with several topologies and structures will be researched in this thesis.

There are several combinations of connecting RESs and ESSs to residential homes that create different engineering challenges and requirements for these inverters. The first most simple type is connecting solar with an inverter directly to the grid with no storage system. Using net metering, the grid provider will credit you for the energy you are putting back into the grid subtracting the amount of energy consumed from the house. [4] GFMs are not a good use for this case since an ESS is needed to take full advantage of the system as solar cells cannot provide energy on command. Another type of house is one with a backup power supply with no RES. This would be something like a certain piece of equipment must remain powered even during an outage. Given that this case is often for maintaining a very important system, they are often isolated from the grid and can be omitted from the scope of this thesis. The next two cases are the two potential use cases are houses that have

both a RES and ESS as a battery, and a house having a RES with a removable ESS like an electric vehicle. This is the ideal use case for a GFM This last case is only recently becoming more common as most EVs up until several years ago, didn't have this capability, but EVs like the Ford F150 Lightning and Hummer EV are now offering access to the high voltage battery to be used with bidirectional chargers to power homes. [5] [6] While there are limitations to this setup since the ESS is not always connected to the grid, a GFM can still be applicable here. The best use case of a GFM is with a RES and a permanent ESS connected to the grid as full capability of the system can be utilized.

An essential part of constructing an inverter that will be connected to the grid is implementing anti islanding protection. "The aim of an anti-islanding protection is to detect grid failures and disconnect generators in order to avoid that the grid is fed in an uncontrolled way." [7] The are several cases that anti islanding protects against; these cases are high voltage, low voltage, high frequencies, low frequencies, and drastic changes in frequency (over 50mHz/s). [7] This is required in systems like solar on houses which don't have control over when the PV is generating energy or not, as well as batteries. Figure 3 shows what the basic circuitry looks like. In certain cases, without this protection, lines that would normally have no power going through them may be live due to a battery or PV which is a large safety risk.

Photovoltaics have varying efficiencies based on the voltage and current on the output, and optimizing this system allows for the PVs to operate near or at their highest efficiency. This process is called maximum power point tracking. This is performed by perturbing the

system and monitoring the response. And using that to find the voltage and current that generates the highest output [8]

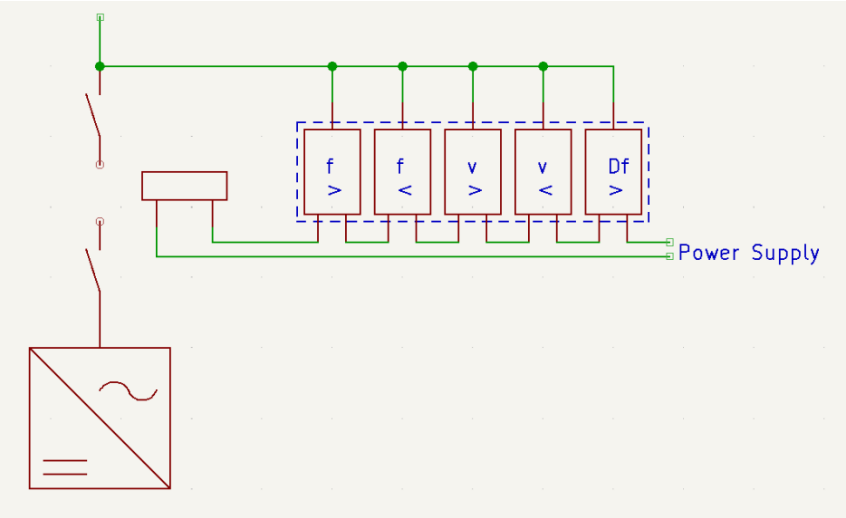

Figure 3: Fundamental Circuit for Anti Islanding Protection System [7]

The output generated on the AC side of an inverter must be filtered as well. The pulse width modulation (PWM) signal generates high frequencies which shouldn't be present in the sinusoidal output. To remove them, a low pass filter is used to isolate the desired frequencies. This is often accomplished with an LC filter, or an LCL filter. [9]

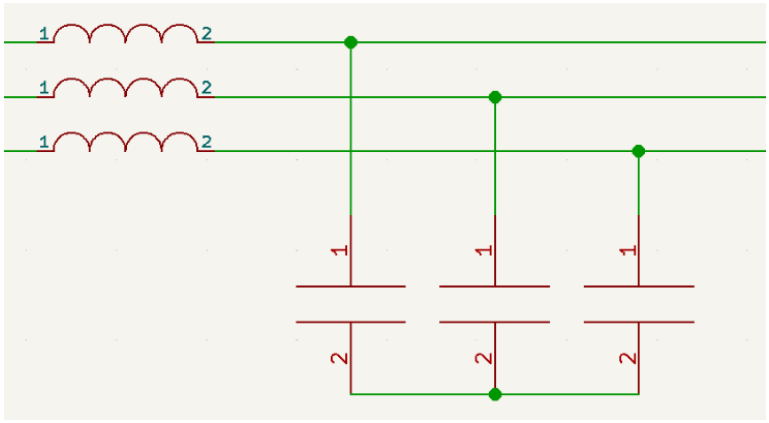

Figure 4: Three phase LC Filter [9]

Figure 4 above shows the general circuit diagram for systems used. Some systems also use an LCL circuit with an additional inductor connected on the output side. It should also be noted that adding more filters to a system while potentially cleaning up the signal also can slow down the response time of the system. [9]

2.3. Wide Band Gap Semiconductors

Wide Band Gap Semiconductors (WBG) are going to play a large role in providing high efficiency power modules for these grid forming inverters in the future. “More than 60% of energy utilized for electricity reproduction is lost during the conversion process” [10] Making these conversions more efficient could save large amounts of money in the future. There are several reasons why WBGs are a good fit for this application. Standard silicon conductors have a bandgap of around 1.12 electron volts (eV) whereas WBGs have a bandgap of over 3 eV. [11] WBGs also can handle much higher voltages up to around 1200v. They also have a much wider range of temperature they can operate in as high as 300 C. [11] Their small form factor also makes them a good fit for applications like electric vehicles and keeping the inverters connected to houses compact. Additionally, WBGs have a wider range of frequencies they can operate with providing additional use cases where regular semiconductors would not be able to be used in. There are some obstacles however as well. Wide bandgap semiconductors can be more difficult and expensive to produce, making them less accessible. Depending on the WGB, they can be very ESD sensitive and easily become defective if not handled carefully. [11]This thesis will reference some of the most relevant WBGs currently being researched and used in some commercial devices.

This includes Silicon Carbide MOSFETs (SiC) as well as Gallium Nitride (GaN) High-electron-mobility Transistors (HEMTs) [12]

Before options like SiCs and GaNs, many devices would use Silicon IGBTs (Si). Si IGBTs are significantly less than efficient in several capacities. One of the most impactful is their low efficiency. Si IGBTs generate much more heat while underload needing a much larger heatsink to dissipate the heat to operate at the required lower temperatures. They also can't handle the large range of frequencies that SiCs and GaNs are able to often, increasing complexity and size of the inverter. SiCs and GaNs can handle much higher voltages as well with SiC handling up to 1200v and GaN handling up to 600v. [13]

2.4. Inverter Topologies

There are several inverter types which will be discussed in this thesis. The process of taking DC voltage from a battery or solar array and connecting them to a house or the grid can be accomplished in various ways with different benefits and drawbacks. The first that will be looked at is the two-level three phase inverter.

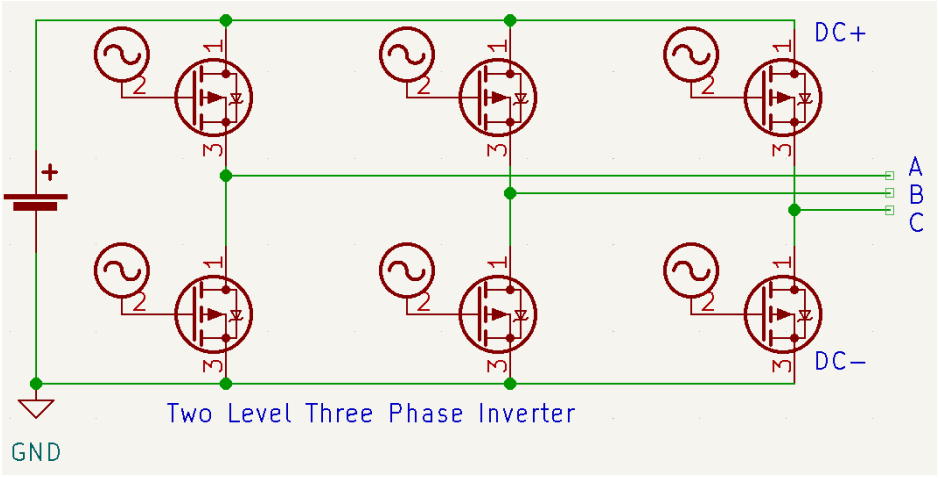

Figure 5: Two level Three Phase Inverter

The image in Figure 5 shows the standard two level three phase inverter. Inputting PWM signals into the six gates to control the output. The three phases, A, B, and C are offset by 120 degrees each. There are several important factors that influence the design of an inverter based on its application. The switch type is important, whether or not an IGBT or MOSFET is used. The voltage and current for the system are also important factors. The environmental aspects must be considered as well. Semiconductors and other components will have different temperature and humidity ranges where they operate at intended. [14] When looking at S1 and S2 in phase A in Figure 5, A certain case needs to be avoided. If both S1 and S2 are switched high at the same time, then a direct connection is created between VCC and ground causing a short. [15] To combat this issue, there is a dead time implemented in between alternating when S1 is high versus S2. During this time, both switches remain off to ensure that there is never a window of time where more than one switch is never on. However, there is a caveat. During this dead zone window, no power is being transferred from the inverter means it generates a reduction in the inverter's efficiency. This creates a tradeoff where the dead zone needs to be a short enough amount of time that the efficiency stays high enough for the use case, but also remains long enough to stay functional and safe. [14] Similar to this topology, three level NPC inverters.

Three level neutral point clamped (NPC) inverters are like two level three phase inverters but provide a different voltage output on the AC side.

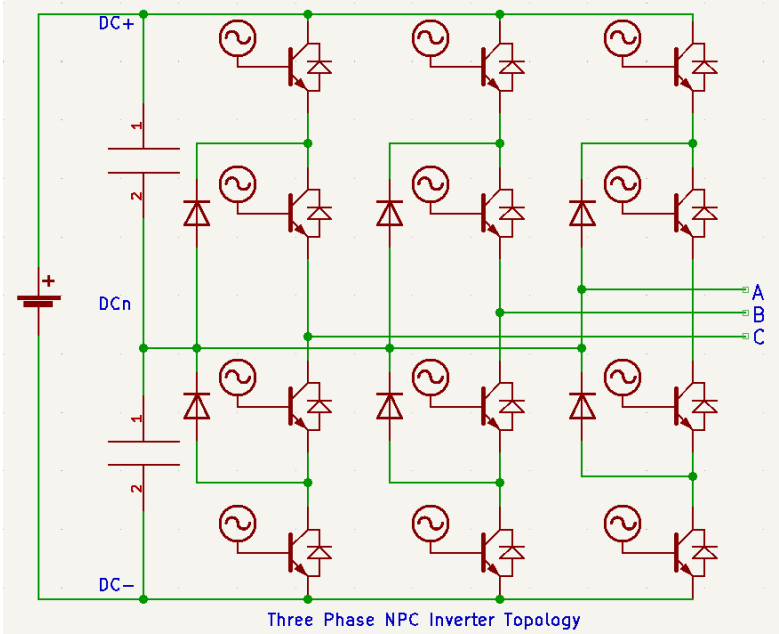

Figure 6: Three phase Multi level NPC Inverter Topology

As shown in Figure 6, there are three voltages available at the output. Unlike a normal two level three phase inverter which either outputs DC or ground, a three level NPC inverter can provide +1/2DC, -1/2DC, or 0v at ground. This is particularly useful in an application that needs the output to be centered around 0v and the output is both positive and negative. One of the requirements for this system is having access to a mid-point of the DC power supply, or two identical power supplies in series. This isn't the only topology that is able to generate these three outputs. Three level T-Type neutral point clamped inverters, rather than implementing diodes, connect half of the switches on the neutral line. Neither of these cases are possible for a battery connected to the house or an EV battery connected, due to the requirement of need access to the voltage at the middle of the DC source, and because of that, won't be considered for the rest of the thesis.

The last inverter topology discussed in this thesis will be High Efficient and Reliable Inverter Concept (HERIC). This design is often used for PV systems.

[16]

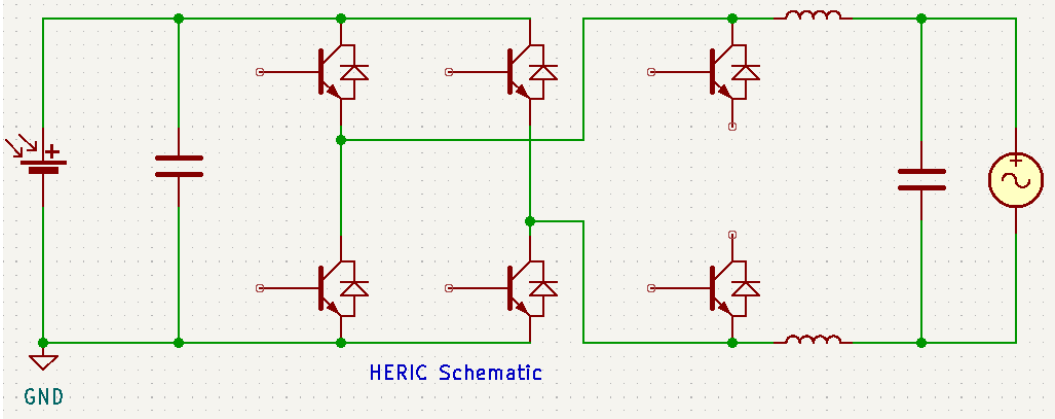

Figure 7: Highly Efficient and Reliable Inverter Schematic [16]

An important factor in inverter selection is taking into account the leakage current generated from it. This happens from several places, most notably transformers. [16] While remaining galvanically isolated, transformer less inverters are becoming common given the development of high efficiency inverters.

2.5. Inverter Control Methods

Inverter control methods play a vital role in the performance and stability of power systems within energy distribution networks. These control methods are used to regulate the power flow between the inverter and the grid, and to maintain system stability by controlling frequency and voltage. The methods that will be discussed in this thesis will include reverse droop control, virtual synchronous generator, and virtual oscillator control. [17] [18] Each of these methods has its unique advantages and limitations and is suited for different applications. [17] In this article, we will explore these control methods and their

applications in detail. There are many other control methods that can be implemented in the future.

There is a hierarchal set of levels for control topologies of microgrids which can be implemented in a system. There are five or six levels to this hierarchy depending on the source, but this thesis will use model described in, "Microgrids in active network management—Part I: Hierarchical control, energy storage, virtual power plants, and market participation," by Omid Palizban, Kimmo Kauhaniemi , and Josep M. Guerrero. [19]

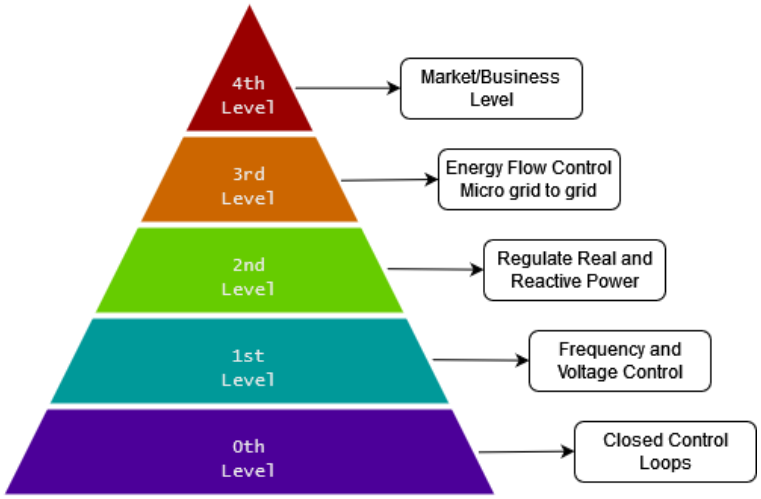

Figure 8: Hierarchical Control Scheme of microgrid

The lowest level of control is level zero in the hierarchical control scheme, shown in Figure 8 above, is the most fundamental and controls the power point of the inverter to control the voltage, and frequency of the system. Having accurate readings for these two values is integral for any system to function properly. However, for this thesis, the focus will be on second level control. [19]

The first level is primary control is the inverter interfacing between the inverter on a house, or a microgrid of sources/buildings. Taking in information such as the state of charge of a battery, load demands or excess in the grid, and the amount of energy being generated by renewable energy sources, the primary control determines the power flow of real and reactive power to keep the network stable. [19]

Reverse droop control, a control method for secondary control systems, offers a good solution for smaller sized distribution generation units. They can help with reduction in transmission losses since energy doesn't have to travel as far from the generator to the load. [20] [21] Reverse droop control operates by changing the real and reactive when load fluctuations are introduced to compensate for them and keep the system stable. One of the benefits of reverse droop control is that it is entirely reliant on the data collected from the grid and communication with other systems is not required. [21] This is very helpful in the consideration microgrids as establishing a connection between every inverter on a grid would be logistically difficult. There may be options in the future for cloud based, or web3 based systems to make this possible in the future.

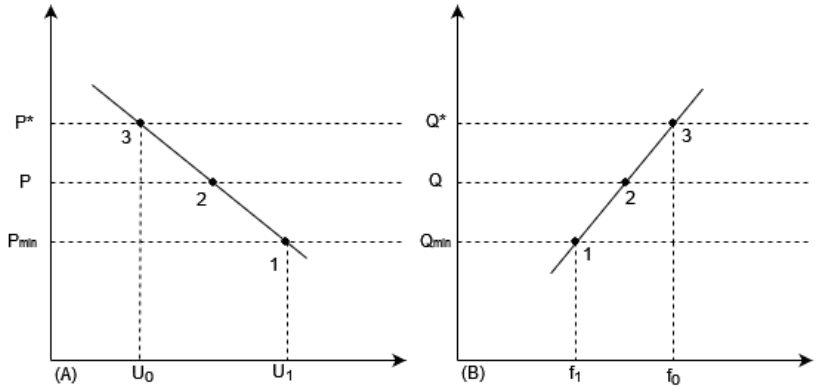

Figure 9: Reverse Droop control characteristics graph. The left side is frequency controlled, and the right side is power controlled.

Reverse droop control actively controls the real power and reactive power individually. Changes in the frequency produce a linear change in the real power as shown in (A) in Figure 9. Alternatively, changes in the voltage result in a linear change in the reactive power as shown in (B) [22]

Reverse droop control increases the power output when the voltage of the power system the inverter is connected to decreases below a certain threshold; it also decreases the power when the voltage increases above a different max value.

$$\begin{cases} P_s^* = P_{s0} - m(U - U_0) \\ Q_s^* = Q_{s0} + n(f - f_0) \end{cases}$$

Figure 10: Reverse Droop-Based Primary Real and Reactive Power Control

As shown above in Figure 10, the reactive power is directly controlled by the frequency. This means an increase in frequency results in an increase of the reactive power and a decrease in reactive power when the frequency drops. The next control method that will be discussed is the virtual synchronous generator. The parameters m and n in Figure 10 define the gain applied to the real and reactive power respectively; this means that a large m value will result in a large change of the real power with the same change in the input voltage.

Virtual synchronous generators (VSG) operate in an entirely different methodology than reverse droop control. VSGs operate by simulating synchronous generators which have many benefits for systems stability given their high inertia and fast response time. [23] Using the power and frequency of the power system the inverter is connected to, VSGs can be used to generate the correct PWM response and control the switches of the inverter. [24] [25] “The control of VSG can be divided into two parts: the outer power loop that

simulates the mechanical characteristic, and the inner current/voltage loop that simulates the electromagnetic characteristic." [23]

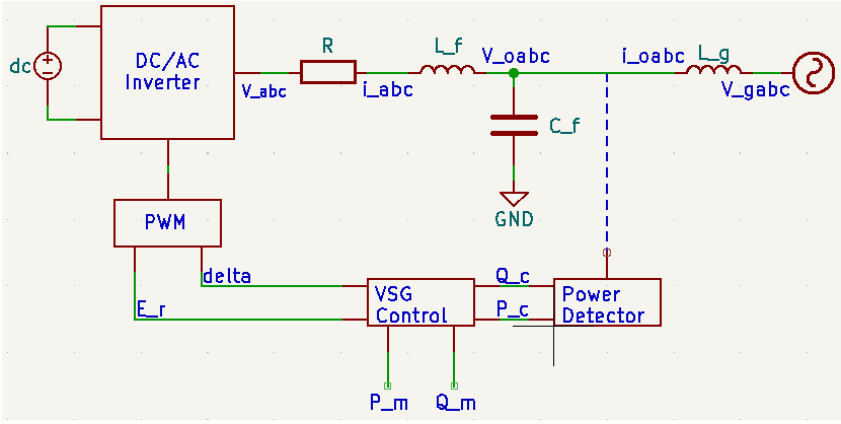

Figure 11: Diagram of Virtual Synchronous Generators

The VSG block is used to determine the voltage and angle on the output that is sent to generate the PWM values to operate the semiconductors. [26] This feedback requires the current power output shown in Figure 11 through Qç and Pc. Real and reactive power both require control to keep the power factor correct. Below in Figure 12 shows the control loop that can be used in VSG. [26]

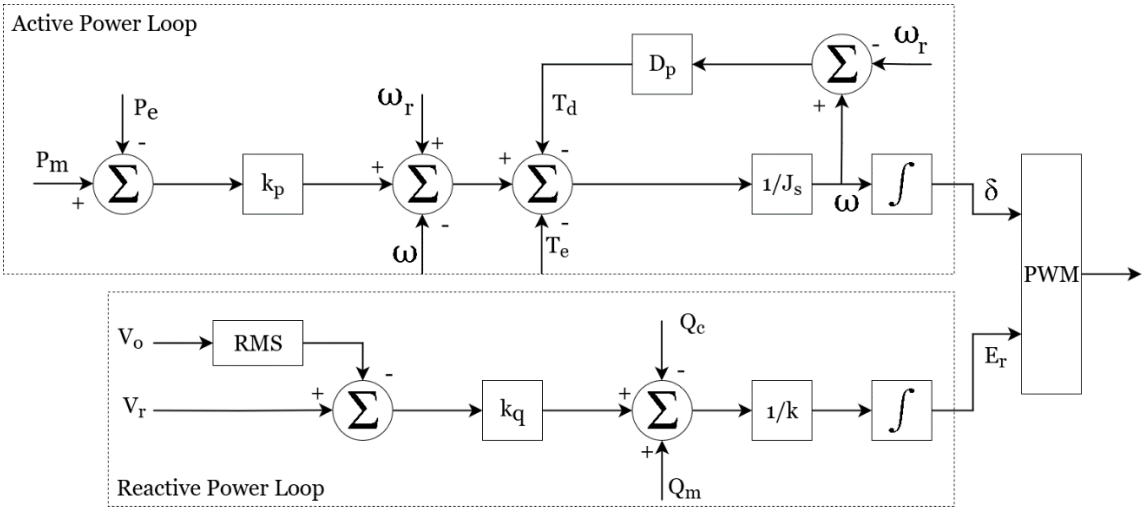

Figure 12: Power Loops for VSG system

Virtual Oscillator Control (VOC) is another alternative method to the primary control of an inverter. VOCs simulate nonlinear harmonic circuits within the time domain, unlike the reverse droop control method which operates within the frequency domain, to create the sinusoidal current needed at the output. [27] by simulating the mathematical phenomenon of coupled oscillators, VOC is able to synchronize with the a supplied The dynamic model for VOCs is given below in Figure 13. [27]

$$L\,\frac{di_L}{dt} = v_c,$$

$$C\frac{di_L}{dt} = -\alpha v_c^3 + \sigma v_c - i_L - k_i i,$$

Figure 13: Dynamic Model for VOC [10]

2.6. Hybrid Inverter Structures

Hybrid Inverter Structures work as the method for integrating PVs, batteries, home appliances, to the three phase AC grid. There are several structures which have varying benefits and drawbacks. They must be directional as batteries will act as a load or generator depending on its state of charge and grid demand. A large part of the design decision is made around the efficiency of converters and inverters; every time a conversion happens, there is a loss of energy so the more times it changes, then the more energy is lost. The goal is producing a system that is stable, efficient, fast responding, and affordable.

The first structure that will be looked at having the battery and PV each have a DC-DC converter that both connect to a DC bus that is connected to an DC-AC inverter which is connected to the grid and circuit breaker. [28] There is another structure that is fairly similar but slightly different which uses a DC-to-DC interface between solar and battery to match

the voltage and uses MPPT connected to an inverter to generate the outputs. This removes the third voltage at the DC bus, but which may be high voltage and potentially dangerous [28]

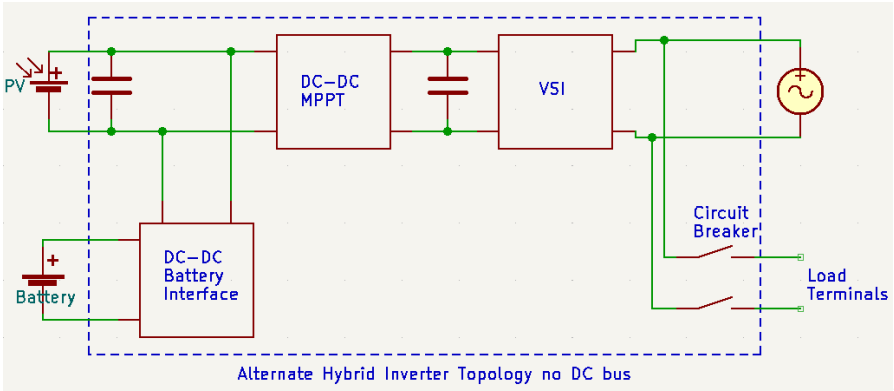

Figure 14: Alternate Hybrid Inverter Topology, no DC bus

This system works very well in the context of DC-DC converters being more efficient than AC-DC inverters as it reduces the number of inverters needed to conserve energy. However, given the recent advances in semiconductor technology such as SiC and GaN, different topologies may be worth considering as well for high power applications.

There are similar topologies with the hybrid inverter not including the isolated DC interface as part of the inverter and requiring that as an additional component before connecting the battery to the system. This could cut down on complexity of the system, but that system will still be needed in the whole hybrid inverter as the DC voltage from the battery will not be the same voltage as the PV system. In the future, more electric vehicles will be connected to the buildings to provide power, and this would not be an option for that case.

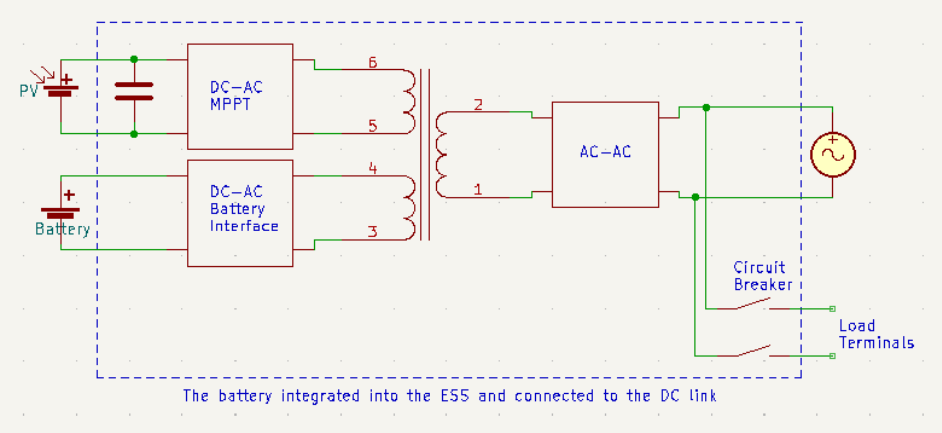

Figure 15: The battery integrated into the Energy Storage Systems and connected to dc-link (ESS)

A model like the one shown in Figure 15 above uses an AC bus with a final AC-AC converter. While having two DC-AC inverters and one AC-AC converter, this option should be reconsidered in high voltage and current potential solutions and will be discussed if they are applicable for microgrid scenarios as well given their benefits. They could lead to more compact inverters on houses, or possibly covering larger complexes like an apartment building.

Chapter Three: Simulations

3.1. Overview

There are many aspects of hybrid inverters that can be simulated. Part of the goal of this thesis is to provide a test base of the system that can be used to simulate as many of aspects of these inverters in one system; this allows for whichever part of the system to be tested and help make decisions such as which semiconductor is most viable given the scale of a system. These simulations will focus on several parts. The first is the control method. These simulations will be run in the Power Simulation [29] A design by Albert Dunford was used as a starting point for the simulation and was modified to fit the purpose of this thesis. [30]

There are many control methods as discussed in chapter 2. This thesis will be simulating several including a base line grid following inverter along with reverse droop control and VSG. The MOSFETs were also simulated individually. This would allow for the testing of how certain MOSFETs would function within a system and provide help in part selection and power requirements of the system; it also can help calculate the power losses of the system and by proxy the efficiency. The system modeled will be a high voltage three phase AC system as that is the most likely application for using high power semiconductors, but the system could be modified to operate in single phase or lower voltage.

3.2. SiC MOSFETS/Grid Following Inverters

The first demonstration will show the efficiencies of SiC MOSFETS using a grid following inverter as a baseline. The MOSFETs implemented are using the level 2 characteristics of the C2M0280120D SiC MOSFET. [31]

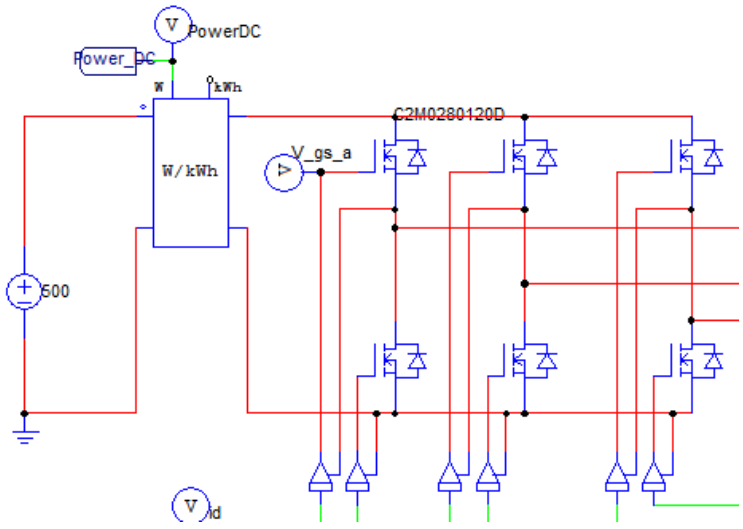

Figure 16: Three phase half bridge inverter

Above in Figure 16 shows part of the simulation of the 3-phase half bridge inverter used to generate the three phase AC power from the DC link that would be provided by solar and batteries as grid forming inverters require an ESS of some kind to provide power to the system. Every MOSFET will have different characteristics.

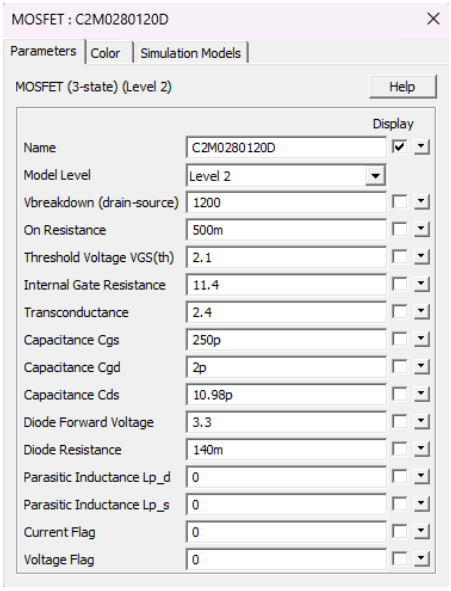

Figure 17: MOSFET Parameters for C2M0280120D

The data shown in Figure 17 is source from the data sheet to simulate the specifics of the C2M0280120D. [31] Alternatively, some manufacturers provide SPICE models of their components, and they could be subbed in here. This would require other inputs such as a temperature input to accurately model them.

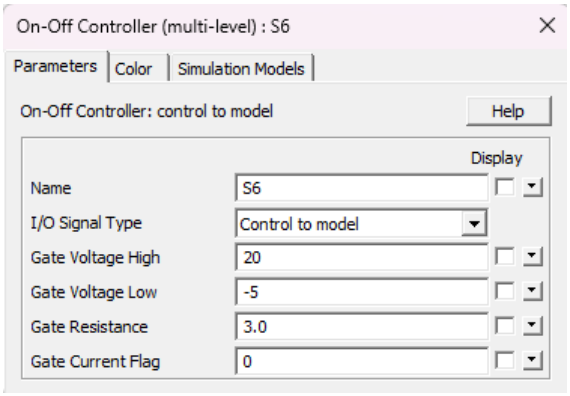

Figure 18: Settings of On-Off Controller

Above in Figure 18 shows the settings used for the on off controller. The high and low voltage are provided by the data sheet and vary depending on the component.

Looking at the difference between the power consumption on the DC side, and AC side can show the efficiency of the MOSFETs in a three-phase system. These inverters are bidirectional and can produce reactive and real power flowing in either direction, but for these tests, the DC system will be providing energy to the AC grid.

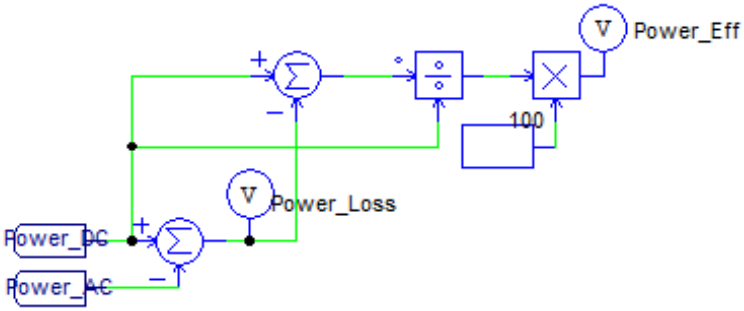

Figure 19: Power Efficiency Calculation

Above in Figure 19 shows the power calculation for the efficiency of the system, looking at the difference between each side. This is from the efficiency equation shown below by $Efficiency = \frac{Power_{out}}{Power_{in}} \times 100\%$. In this case, the difference is calculated, then subtracted from the output power. This can also be done by dividing the output directly with the input, however was used to also provide the loss power.

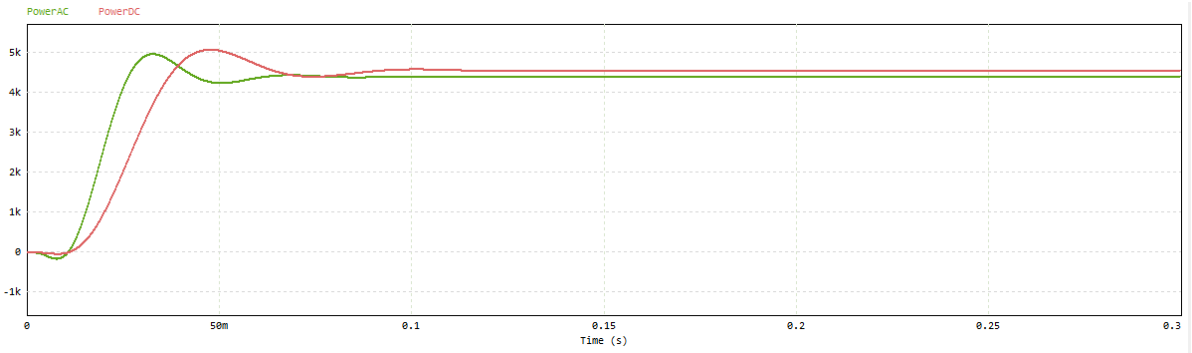

Figure 20: Power on DC and AC Side

Processing the data in Figure 20, the efficiency of the system can be calculated.

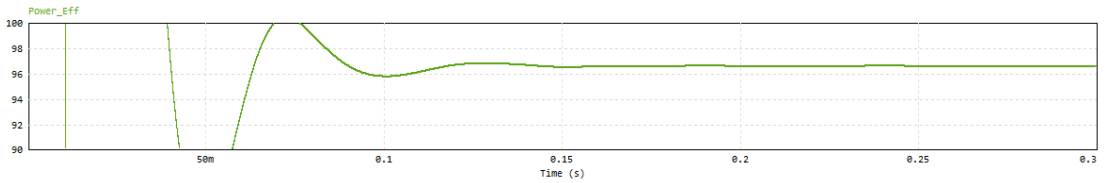

Figure 21: Efficiency of Inverter

Figure 21 shows that, when the inverter reaches steady state, the C2M0280120D in a three phase have an efficiency of roughly 96.7%. The MOSFET can be replaced with another SiC MOSFET that will be used for building the actual inverter that tested. This is the CCB021M12FM3 WolfSpeed Module. [32]

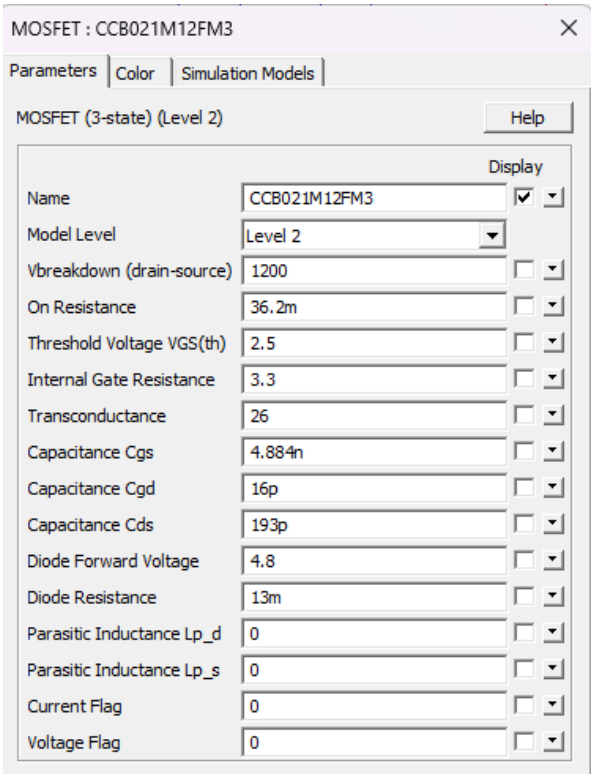

Figure 22: MOSFET Parameters of CCB021M12FM3

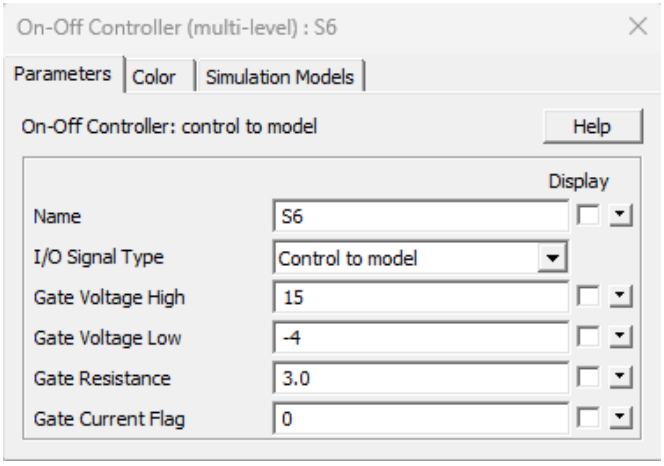

Figure 23: On-Off Controller Setting for CCB021M12FM3

Figures 22 and 23 provide the inputs for CCB021M12FM3 gathered from the data sheet. [32]

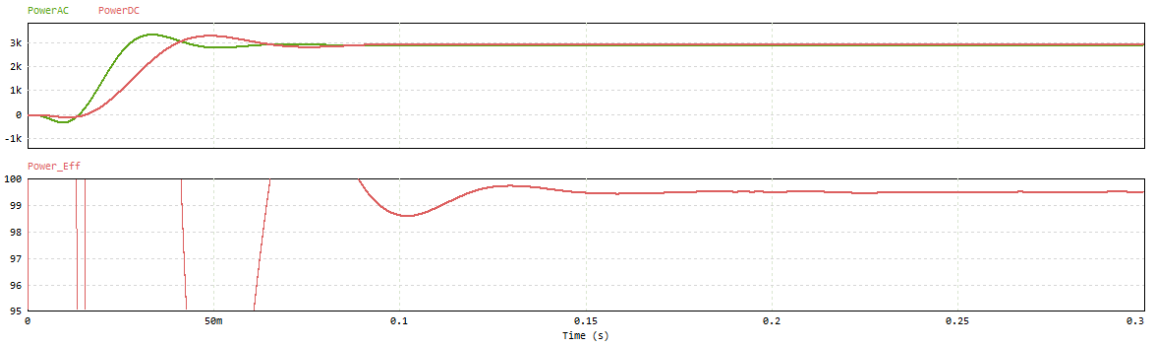

Figure 24: Outputs for CCB021M12FM3

The CCB021M12FM3 only loses around 62W generating almost 3000W producing and efficiency of roughly 97.9%. The entire grid following inverter diagram looks like Figure 25 on the next page.

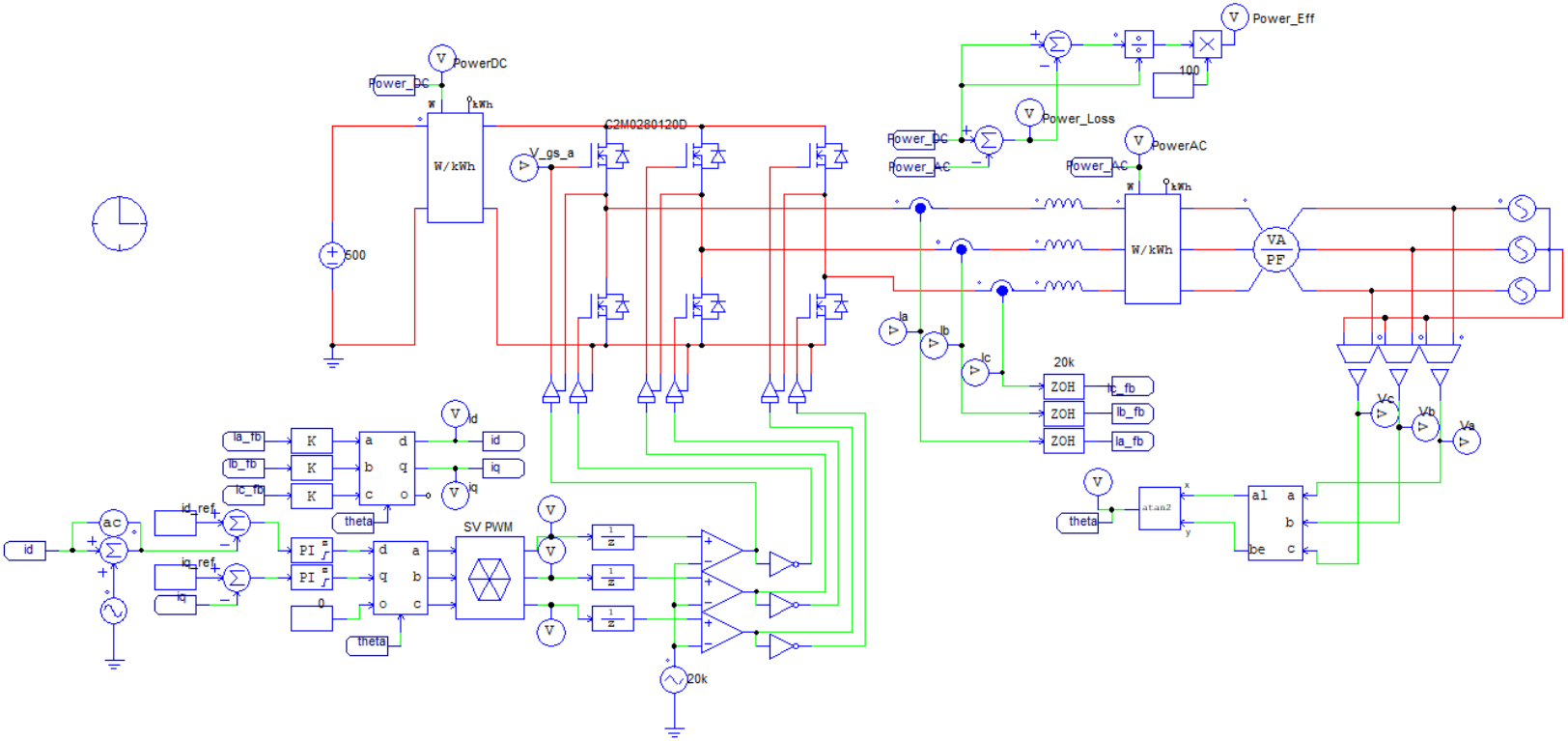

Figure 25: Grid Following Inverter Using SiC MOSFET in PSIM

Figure 25 is the full system of the grid forming inverter that was tested. This system looks at the current on the AC side connected to the grid and synchronizes with it. It is unable to control its frequency or voltage. This is different compared to grid forming inverters that will be compared in the next parts of chapter 3.

3.3. Reverse Droop Control Simulation

For consistency of comparison, the different control schemes for grid forming inverters that will be tested will all be using the CCB021M12FM4 WolfSpeed Module. This is also the module that is being used for real system testing. The first control method that will be looked at is the most common method for hybrid inverters which is reverse droop control. As stated in chapter 2, reverse droop control uses the voltage and frequency of the AC system. It is connected to alter the real and reactive power on its output respectively. The voltage impacts the real power with the frequency impacting the reactive power. By using a phase locked loop, the frequency, and real component of the voltage can be extracted and processed to provide a gain to the real and reactive power.

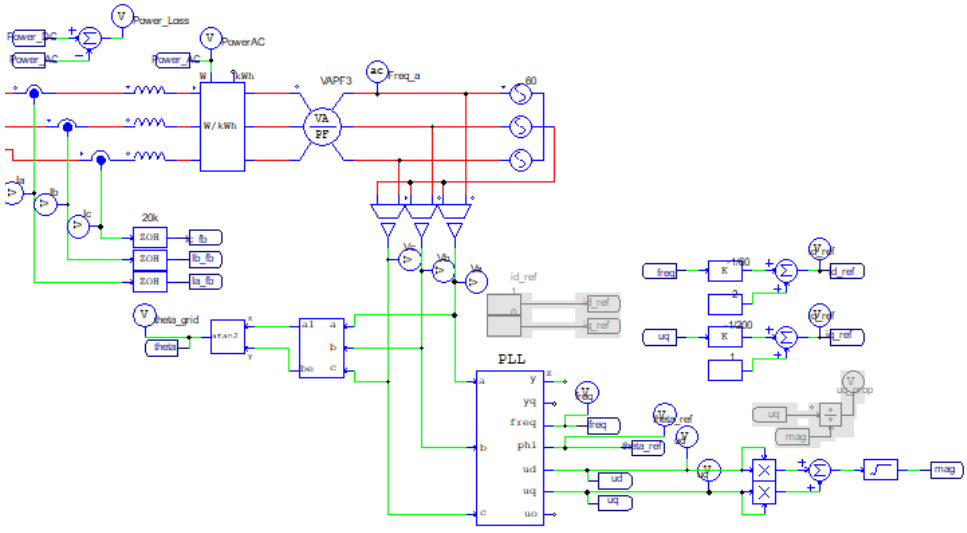

Figure 26: Grid Forming Inverter Diagram with Reverse Droop Control

Figure 26 shows the implementation of reverse droop control. The first step is taking the three phases, a, b, and c from the grid and inputting them into the PLL system. From here the frequency and magnitude of the voltage are generated.

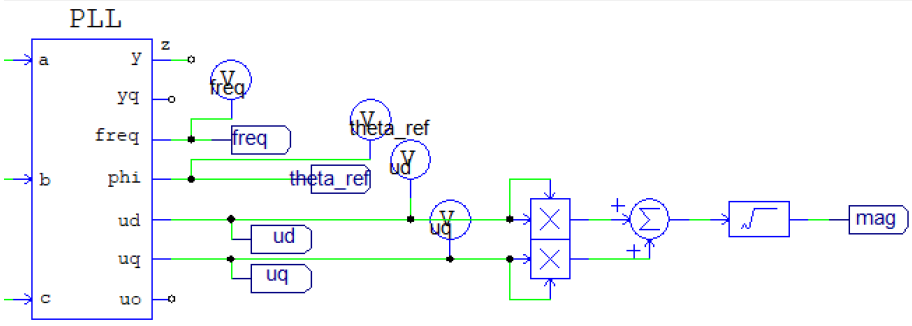

Figure 27: Phase locked loop input into reverse droop control

The next step is applying a linear gain to the real and reactive power of the system.

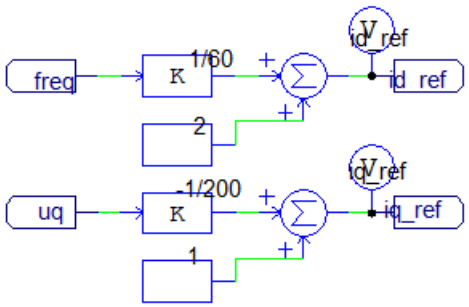

Figure 28: Generating gain for power input

Figure 28 above shows the gain generated around the reference values. In this simulation, the power flow is kept constant going from the DC side to the AC side.

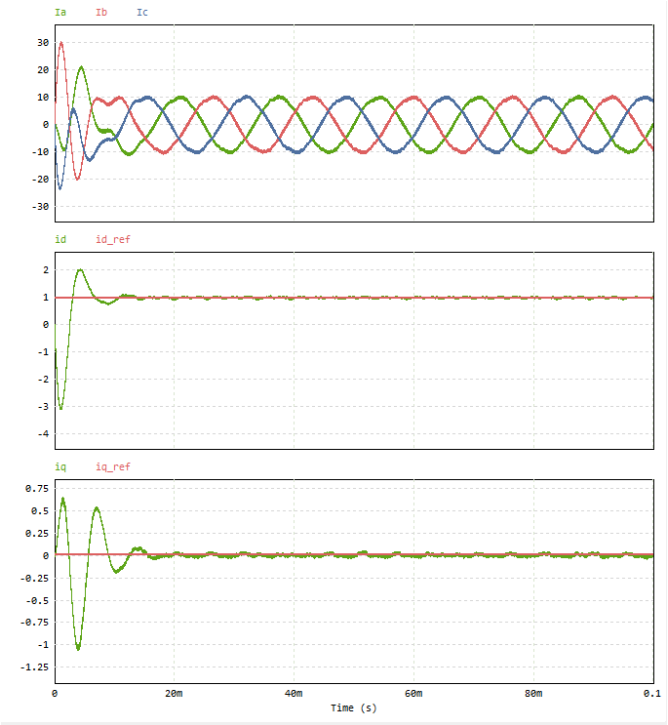

Figure 29: Outputs for Reverse Droop Control System

Above in Figure 29 shows the current output of the inverter which is able to synchronize with the grid. Id and Iq in Figure 29 are the real and reactive components of the 3-phase system and here it is shown that the they converge in roughly 20ms along with

the current. These values are then passed to the rest of the system to generate the PWM values to control the MOSFETS. A Virtual Synchronous Generator model was tested next.

3.4. Virtual Synchronous Generators Simulation

Virtual Synchronous Generators simulate another 3-phase system and uses that

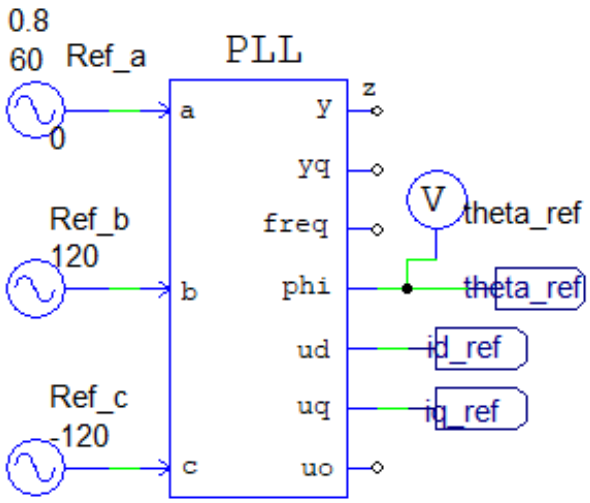

Figure 30: Simulated 3 phase reference

This reference is then passed the control system shown in Figure 12 to produce the desired PWM signal on the output.

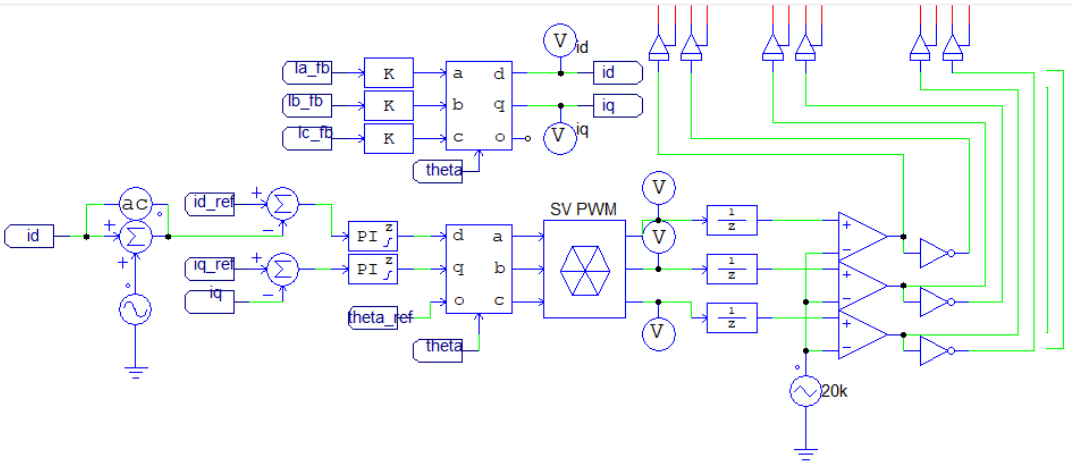

Figure 31: Three phase version of the control scheme shown in figure 12 for VSG

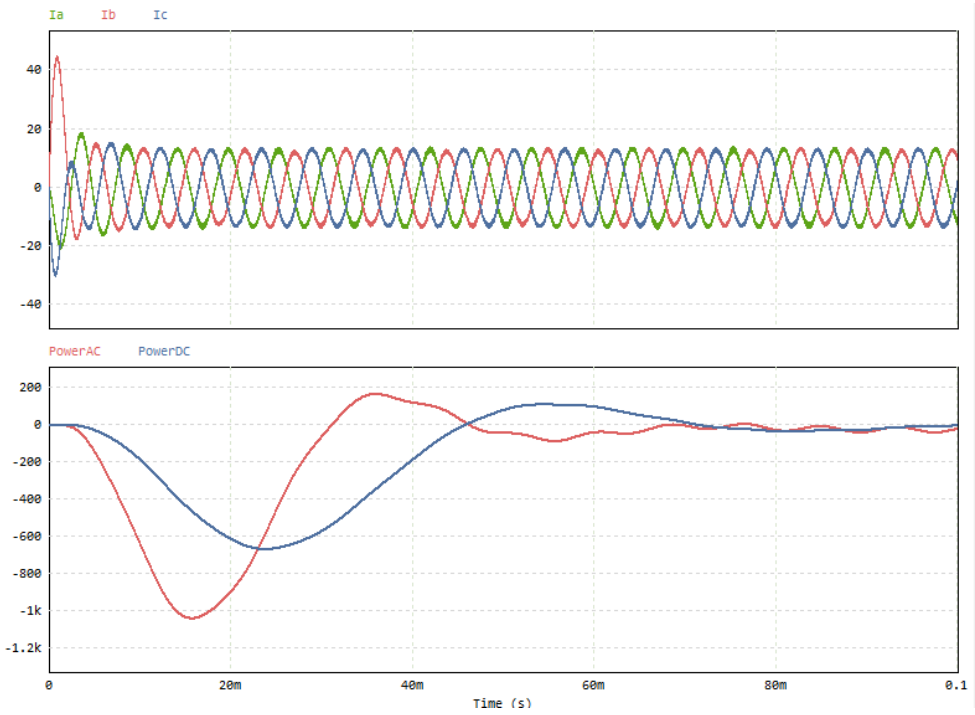

Figure 31: VSG Outputs

Figure 32 shows the resultant power characteristics of the VSG system. As shown, it takes roughly 70ms for the power of the system to stabilize.

This chapter has shown that multiple facets of the hybrid inverter are able to be simulated using PSIM to help as a tool in developing inverters for microgrid settings. There are many moving parts to these systems and all of them can have impacts on the efficiency and response times of the system. They can also have large impacts on the electrical and computational complexities of the system. There are many more combinations that can be tested and validated with this system for future research as well. The next chapter will dive into the physical system developed of a power stage and gate driver of a three-phase inverter.

Chapter Four: Inverter Development

4.1. Introduction

Working with the University of Augsburg. During the 2021-2021 academic year, an inverter was developed. An article was also published in IEEE Electrification Magazine, consisting of Carsten Markgraf, Luca Gacy, Samuel Leitenmaier, Daniel Lengerer, Benjamin Schwartz, David W. Gao. [33] There were several parts of this inverter which will be briefly mentioned but the focus will be on the power stage and gate driver. These additional areas include the control method, controller board, as well as the cooling system. The first step to building a power stage and gate driver module is defining the requirements of the system. Once the requirements for the system have been established, component selection can begin; based on the needs of the system, specific pieces will be used to construct the full schematic and PCB of the system. When the system has been built, the parts can be purchased along with the PCB fabricated. After soldering all the components and testing each subsection, the system can be tested. [33]

4.2. Requirements

The requirements of a system define how it will be constructed since each use case will alter the decisions making process. For the inverter required by the University of Augsburg, they were the following. The inverter must be a three-phase system as well be bidirectional. The inverter must be able to handle on average 20kw and up to 36kW at peaks. The output

must be variable from 0 hertz up to 1200Hz with a carrier frequency of 8kHz. The system must be isolated as well. This means keeping the lower power logic part of the system, galvanically, or optically isolated. This separation keeps the often more expensive control system in case of a fault or failure on the high-power side. The system also needs several points of feedback for the control system to work at its maximum efficiency. This includes a temperature sensor in case the power module exceeds the rated temperature, as well as the current on each phase for a close loop system. All these parts must communicate with the established system by the team at the University of Augsburg. A 24v power supply is used for the low power side, and the desired signal generated at the output of the inverter is provided by a 3.3V PWM signal with an 8khz carrier frequency as specified earlier. The thermistor along with the current sensor both output 3.3v analog outputs which are provided to the control board. The output voltage must handle up to 600V with peak current draw of 60A. The form factor must remain compact and fit within the dimensions of 14 x 5 x 8 in. With the requirements of the system established, component selection can start. Figure 32 below shows the system that will be designed and manufactured within the scope of the thesis. The parts outside the red border show the sections built by the team from the University of Augsburg or parts already on the existing system. [33]

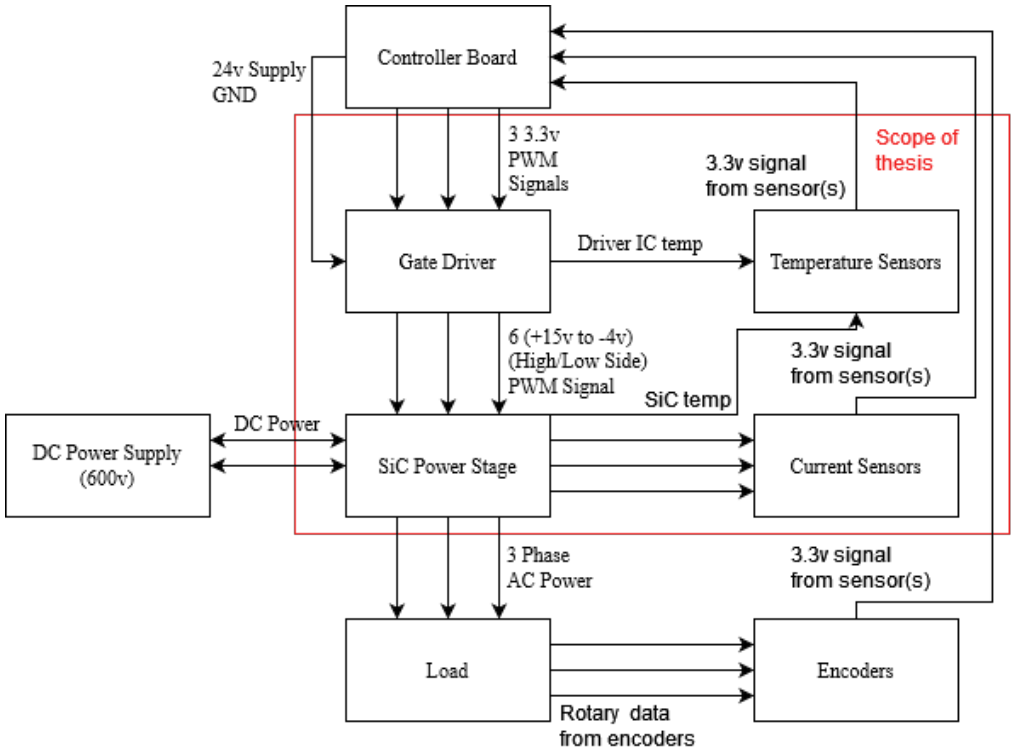

Figure 32: Block Diagram of Inverter System

The two modules that need to be designed are the gate driver and the power stage. They each have their own requirements and PCBs. Below are the diagrams for each system in Figure 34 and Figure 35. [33]

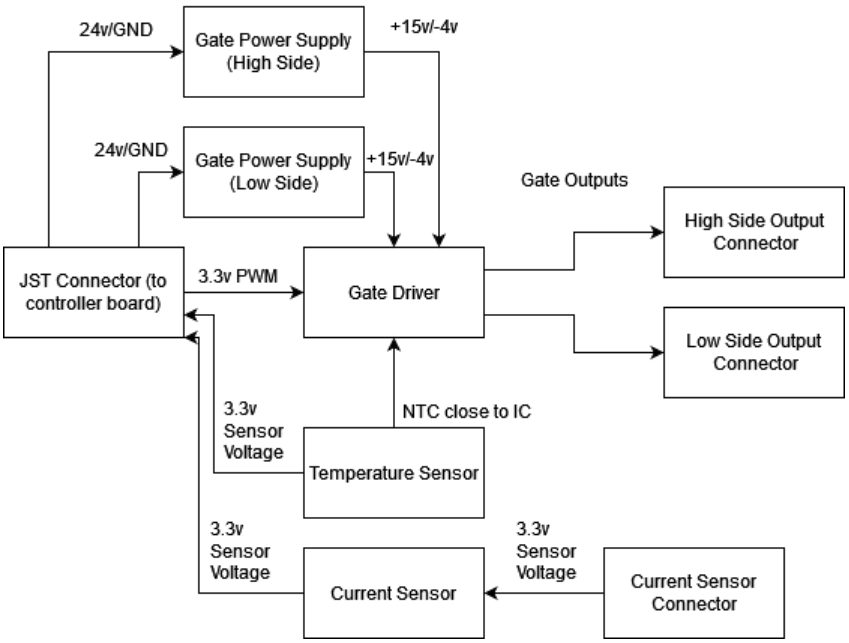

Figure 33: Gate Driver Diagram Single Phase

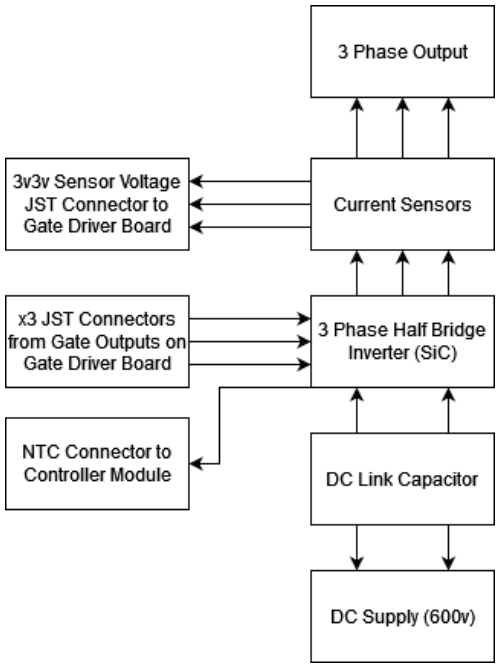

Figure 34: Power Stage Diagram

4.3. Component Selection

The most important part of the inverter component selection is the semiconductor used for the power module. As discussed in the section regarding wide bad gap semiconductors, the requirements decide which best fits this inverter. The two options between SiC and GaN have several determining factors but the SiC ends up being the desirable choice for this case. Despite both GaN and SiC being able to handle the required voltage needed, the wider temperature range along with the ability to handle higher current spikes that SiC modules is best option. WolfSpeed has SiC power modules designed for solar and drive trains which provide, and the CCB021M12FM3 fits all the requirements well. [34] A difficult part of this process was navigating around the chip shortages that were present during the time of development of the boards. [33]

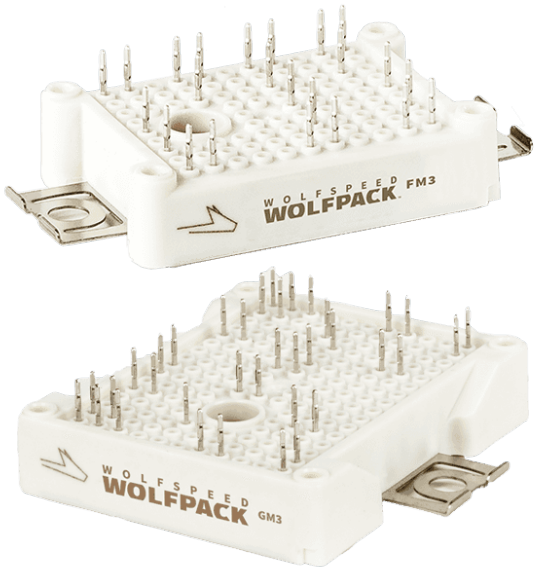

Figure 35: CCB021M12FM3 WolfSpeed power module

This module is a three-phase half bride inverter which can be used to generate the three-phase. However, SiC MOFETs don't operate at the voltages provided and require a DC link capacitor, gate driver, as well as power supplies.

The DC link capacitors are used to stabilize the DC link voltage on the high side of the inverter. [35] This value can be calculated based on the parameters of the system.

$$C = \frac{I_{rms}}{V_{ripple} \cdot 2 \cdot \pi \cdot f}$$

$$C = \frac{60/\sqrt{2}}{10 \cdot 2 \cdot \pi \cdot 8000} = 84.4\text{uF}$$

Figure 36: Equation for calculating the DC Link Capacitor value for Film Capacitor [35]

The equation above shown in Figure 37 shows the equation to calculate the capacitance of a film capacitor. Based on the parameters of this specific system, the needed value ended up roughly 80uF. However, 80uF capacitors able to handle the required voltage of the system at the time of sourcing parts proved expensive with long delivery times, so four 20uF capacitors were used. The Kemet C4AUJBW5200M3FJ was used in this inverter. [36] [33]

Since SiC MOSFETs operate at different voltages with 15v and -4v, a gate driver IC is required which is also able to provide points of protection and functionality. The IC's

isolation is rated at 5700Vrms which is more than enough for this application. It also has undervoltage lock out as well as variable dead time. [37] [33]

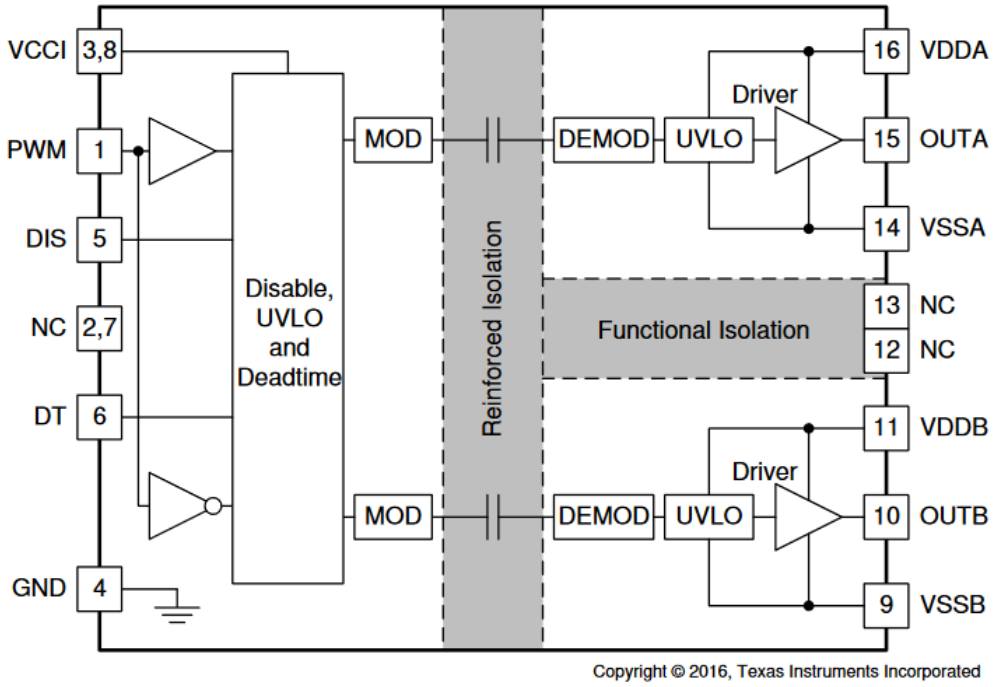

Figure 37: UCC20520 Function Block Diagram

This dead time is controlled by pin 6 on the IC through connected a resistor of a specific value, or a potentiometer to manually adjust the dead time the equal to ten times the resistance connected in nanoseconds. The parameters such as operating voltage range along with the PWM input are compatible with the control board to easily communicate to each other.

There are several different voltages at different points of the system which need converters to use the given 24v and 3.3v output from the controller. The gate driver can operate between 3v and 18v so this can use the 3.3v provided from the controller. However, the SiC MOSFETs require +15v and -4v. This also needs to be isolated. This was

accomplished by using a RSOE-2405SZ/H2 which can take in between 9v and 36 to output 5v at 1W with 2kV of isolation. [38] which is then converted to +15V and -4V with a converter circuit shown below. [39] [33]

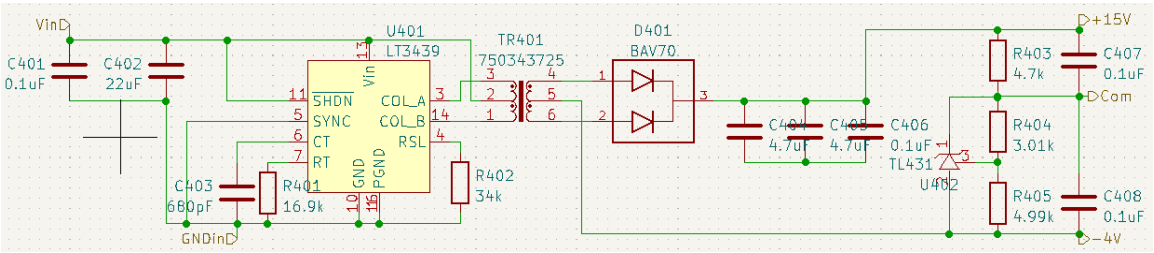

Figure 38: Isolated Power Supply Circuit

For measuring the current, an isolated ACS770xCB-150B-PSF produces a voltage correlating to the desired current and generates a 3.3output which is sent to the controller board for feedback. This has the needed amount of isolation as well as temperature range for the system. [40] [33]

Temperature sensor is utilizing a thermistor in a voltage divider circuit with a 3.3v max to generate a scalable signal that can be sent to the controller board.

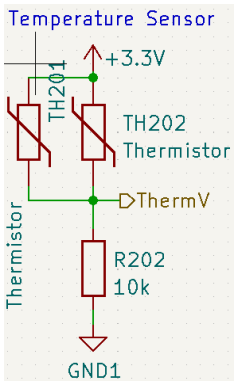

Figure 39: Temperature Sensor Circuit

The two thermistors in parallel are to provide options surface mount along with a through hole alternative. The through hole was used to provide variable placement of the thermistor

in testing. This is for measuring the temperature of the gate driver board to make sure it is operating within its valid temperature ranges. There is also a thermistor connected to the SiC MOSFETs which was provided an output as well to the controller board. [33]

With the components picked out, the design of high voltage and current was able to be completed.

4.4 High Power PCB Design

The copper traces on circuit boards of specific thickness and width are able to handle a max current defined by the equation below. [41]

$$I = K \cdot \Delta T^{0.44} \cdot (W \cdot H)^{0.725}$$

Figure 40: Formula from IPC 2221 for max current of traces

The output is max current in amps. The delta T is temperature rise above ambient in C. W is the width in mils, with H as the height in mils. K is 0.024 for internal traces and 0.048 for external traces. Based on the requirements, and size limitations an 8-layer board with a thickness of 0.25 in was chosen.

4.5. Additional Components

With all the design decisions made above, the full schematic can be built in KiCAD 6. [41] Two boards were manufactured for this inverter, the gate driver board holding all the low power electronics which is connected to the power module and controller board through JST connectors. This board contains the line of isolation protecting the controller board from the high side system. The power module is connected to the gate driver board, along with high power DC voltage system, which is either a battery or solar panel, with the three-phase output connected to the grid of a motor. [33]

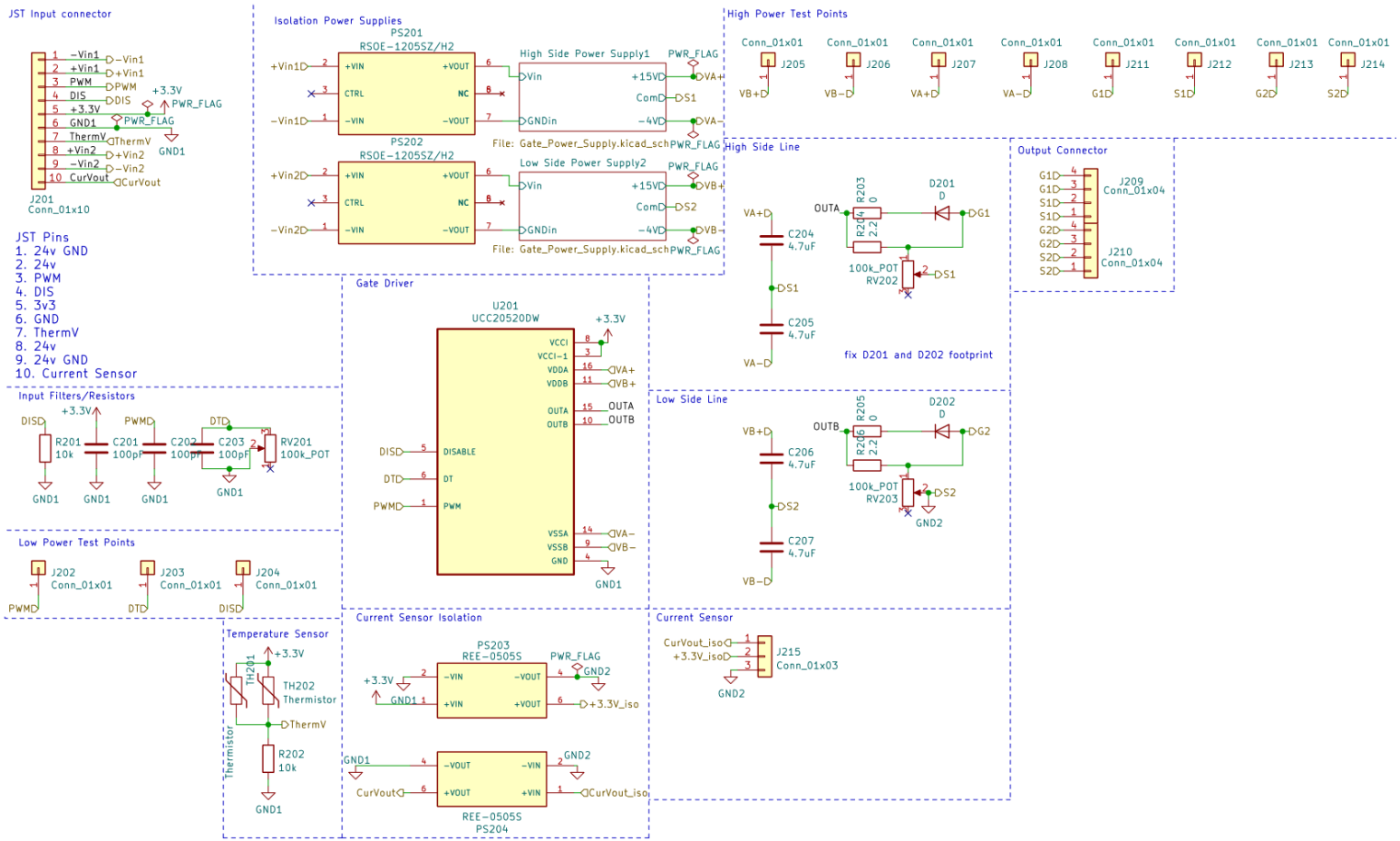

Figure 41: Schematic of single phase of gate driver board

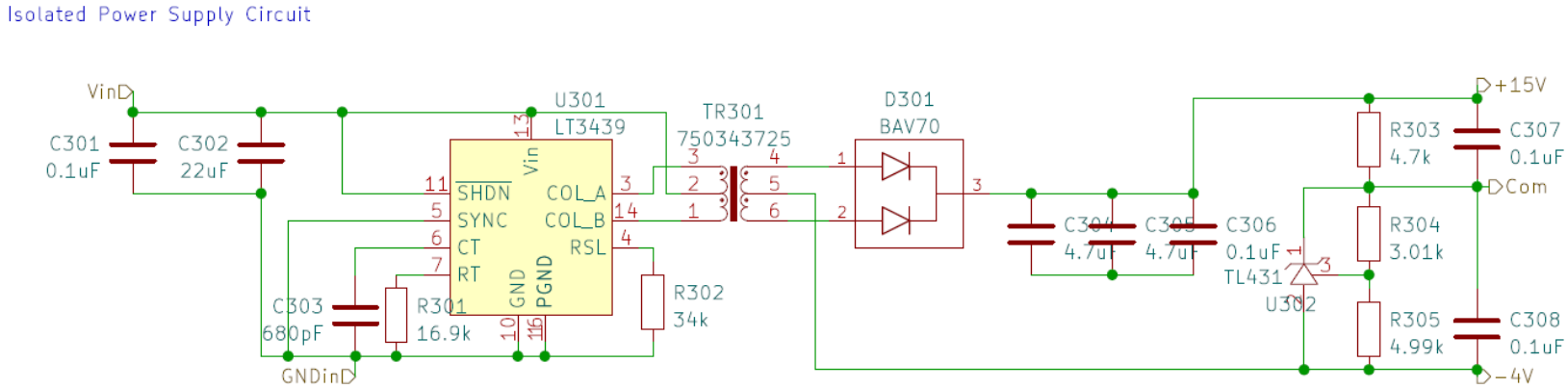

Figure 42: Isolated power supply circuit (Same for high and low side) subcircuit

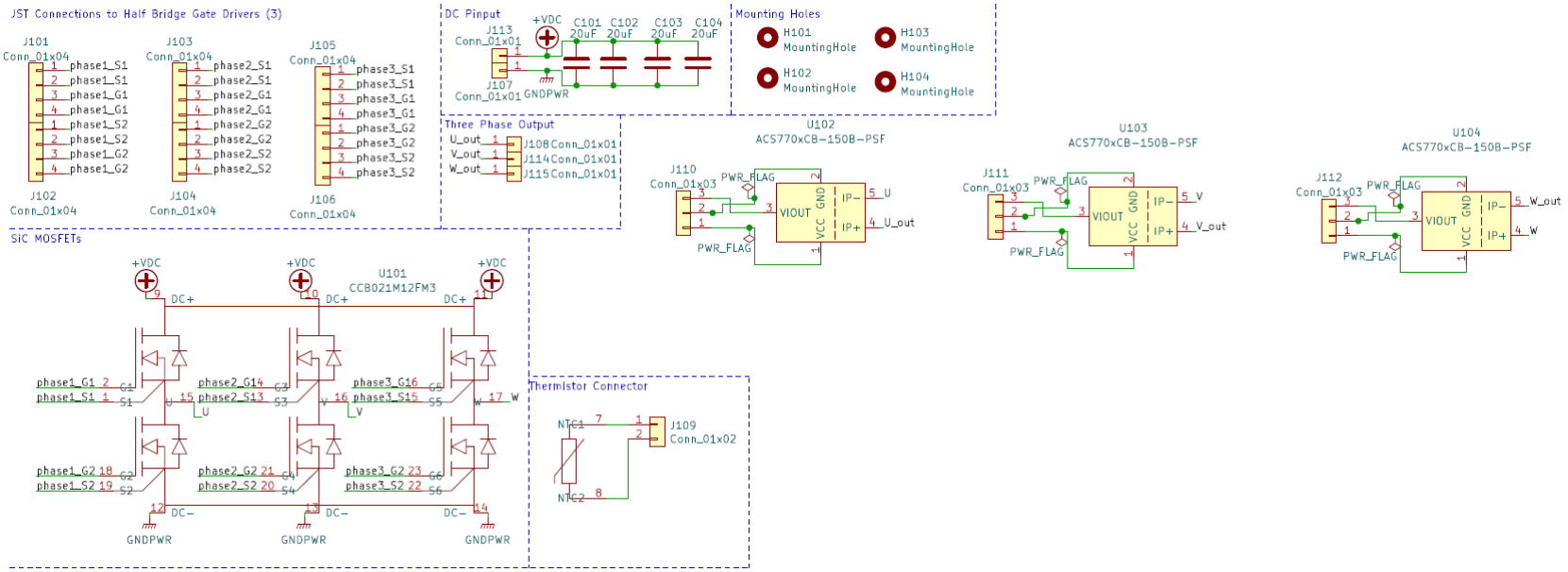

Figure 43: Power Stage Module Schematic

The three schematics above make up the inverter in two main parts. Figure 42 shows the main gate driver module schematic that is divided off into its areas which are labelled in the top left corner of each section. The high and low side power supply subcircuits in Figure 43 are shown with their respective inputs and outputs. The schematic shown in Figure 44 shows the power stage schematic. With the schematic fully defined the PCB can be designed. [33]

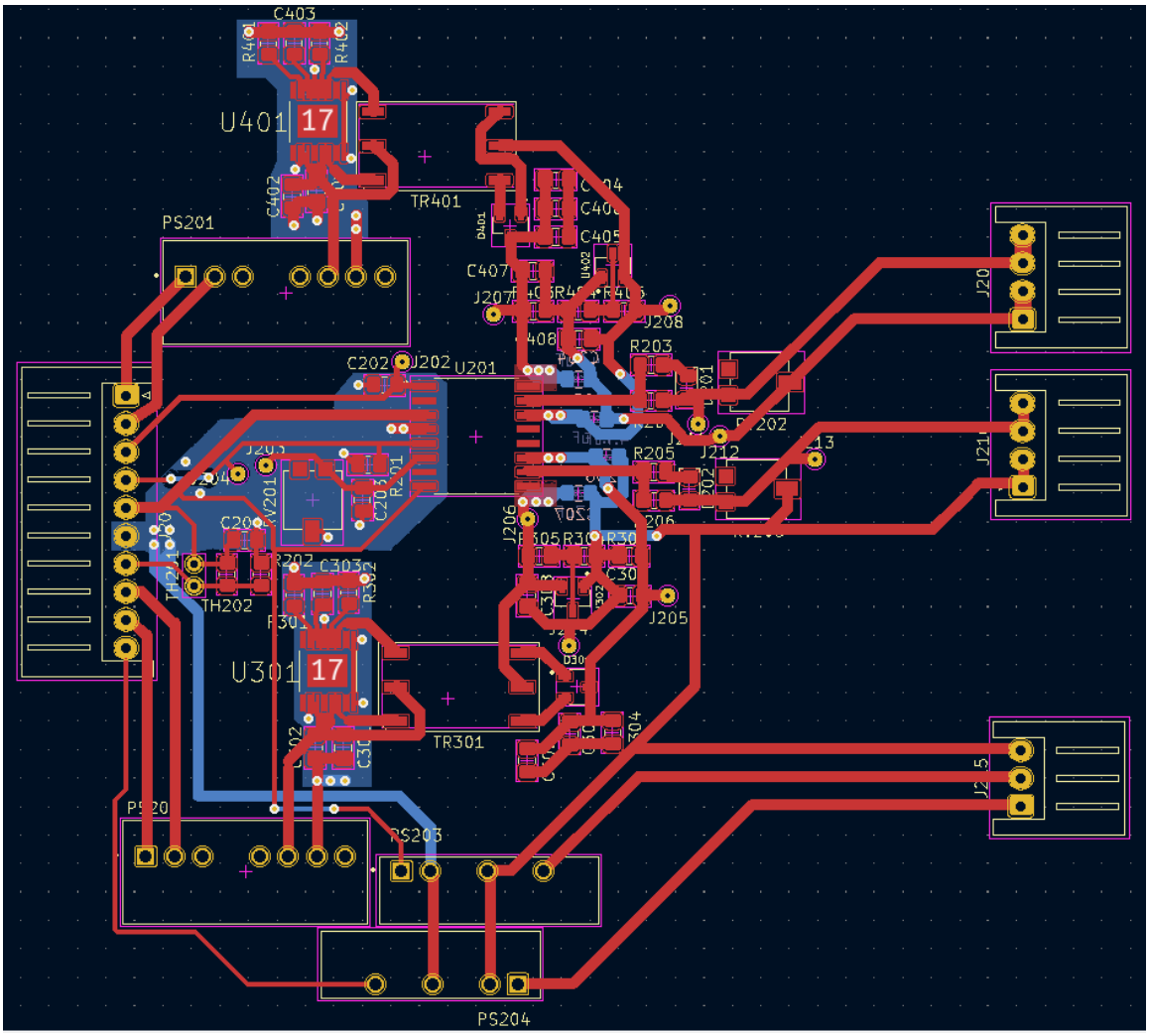

Figure 44: PCB for single phase of Gate Driver Board

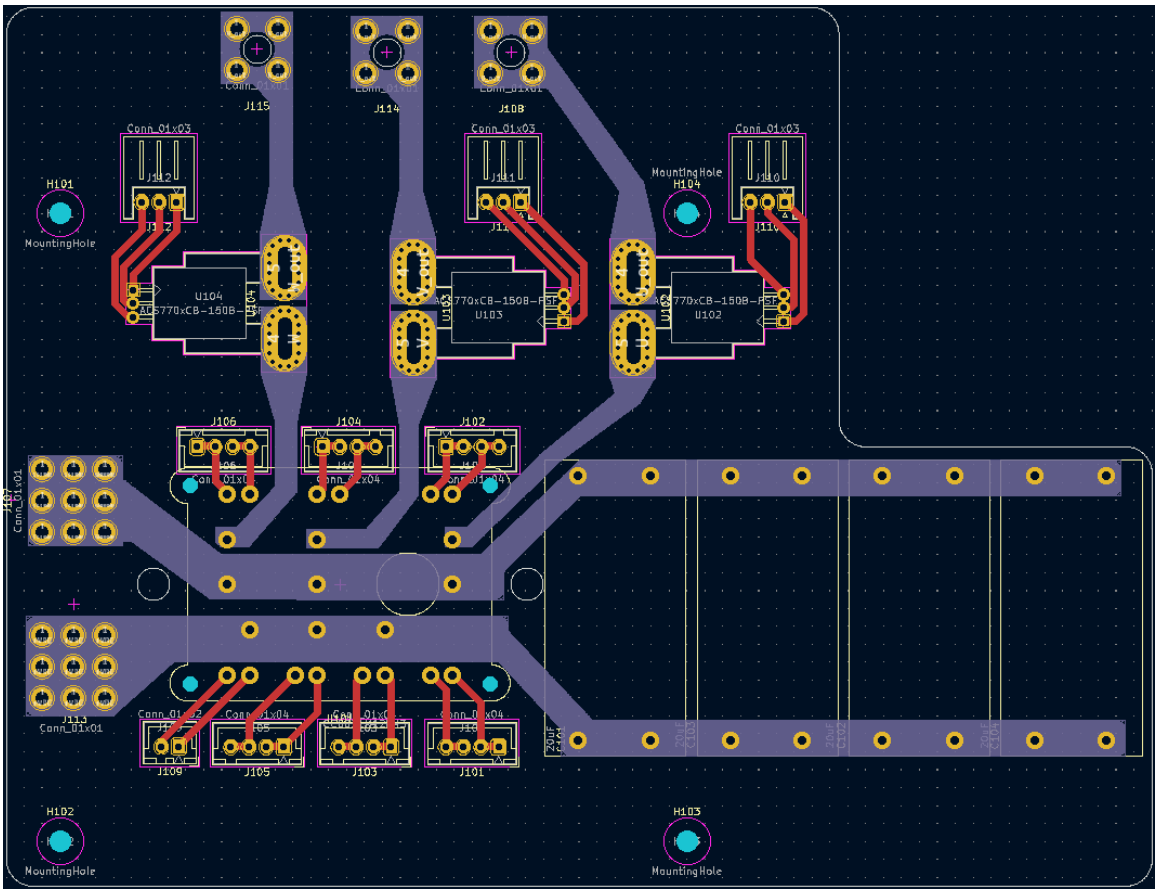

Figure 45: PCB for Power Stage Module

The PCBs shown above in Figure 45 and Figure 46 are the gate driver PCB and power stage PCB respectively. The blue parts of Figure 46 are the eight layers stacked on top of each other and red traces are on the top layer.

4.6. Results

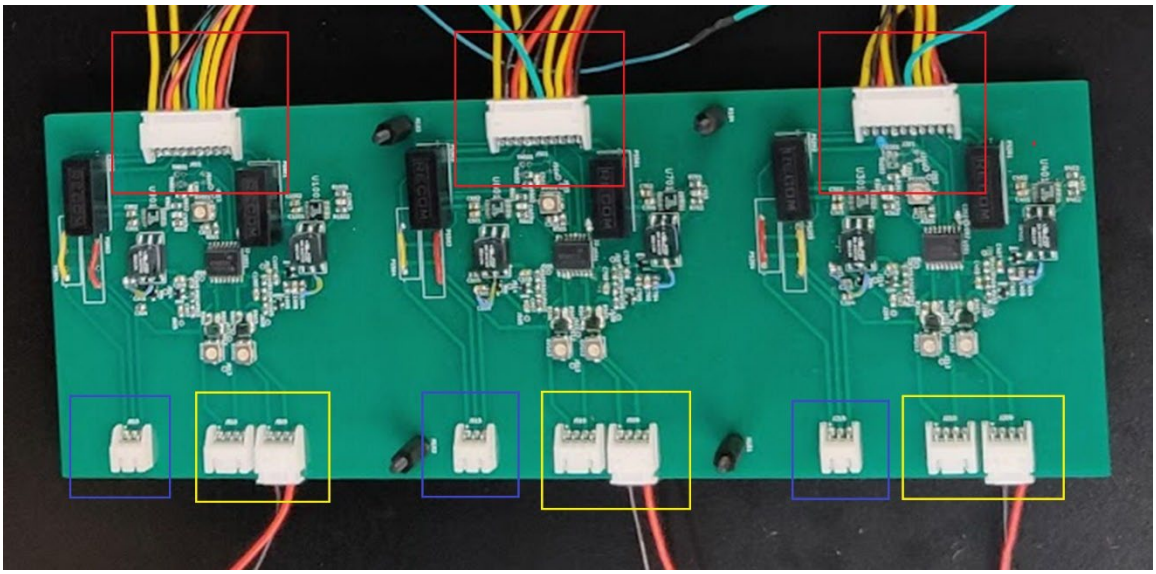

Figure 46: Fully Assembled Gate Driver PCB. The red sections are the connections to the controller board, the blue is the connector for the current sensor on the power stage, and the yellow is the high and low side of the output of the grate driver that is connected to the gates of the SiC MOSFET on the power module.

Above in Figure 47, is the fully assembled and tested PCB for the gate driver. This is connected to the controller board shown at the top of the board, and the power module on the bottom half. Only the high side of each are connected in this image as the outputs are plugged into an oscilloscope and the low side is simply the inverse of the high side. [33]

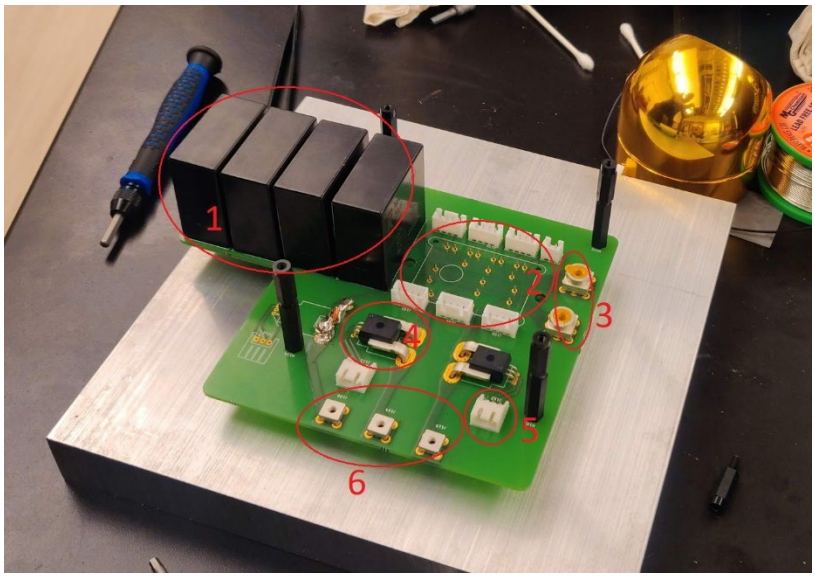

Figure 47: Fully Assembled Power Stage PCB. Section 1 is the DC Link Capacitor bank, section 2 is the SiC MOSFET Module (mounted underneath), section 3 is the DC Voltage Connectors, section 4 are the current sensors, section 5 is the connector for the current sensors, and section 6 is the 3-phase output connectors.

With each subsystem tested, the whole system is ready to be tested. Below in Figure 48 shows the system completely wired up. Due to limited quantities of parts, only two current sensors were able to be sources, so the last phase has a bus wire soldered in its place. [33]

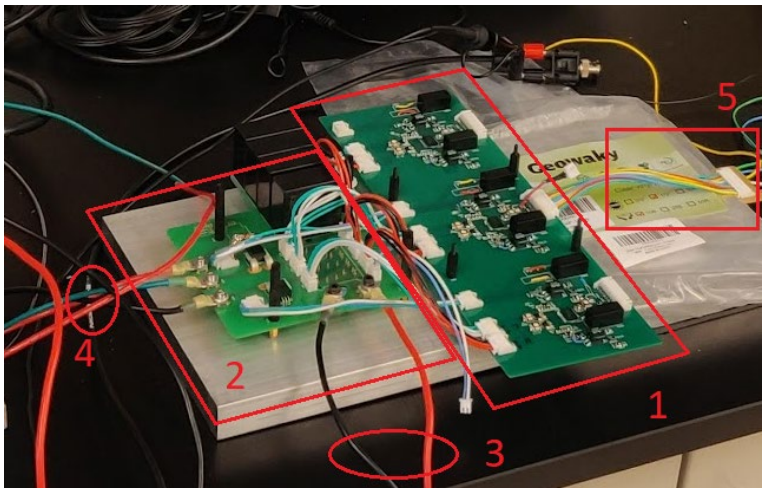

Figure 48: Fully wired-up system on test bench. Section 1 is the gate driver, section 2 is the power stage, section 3 is the DC Input connected, section 4 is the 3-phase output, and section 5 is the connection to the controller board (only One phase connected in the image during testing)

With the outputs connected, not under load, to an oscilloscope the output on one phase showed the following data:

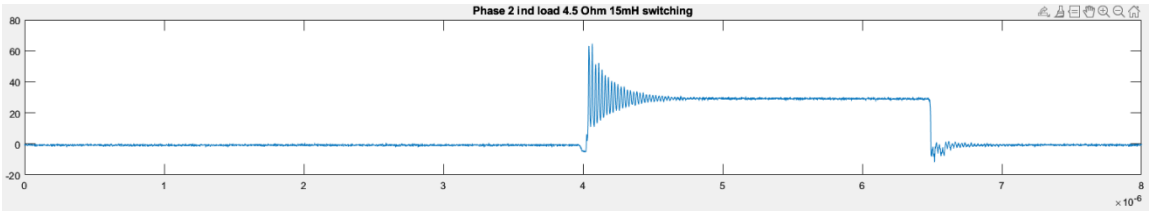

Figure 49: Signal of one period of PWM output

There is some ringing present, and this could likely be solved in a future version using an LC circuit to remove the higher frequencies. This single-phase output was tested underload. In order to see the thermal response of the system, a thermal camera was used.

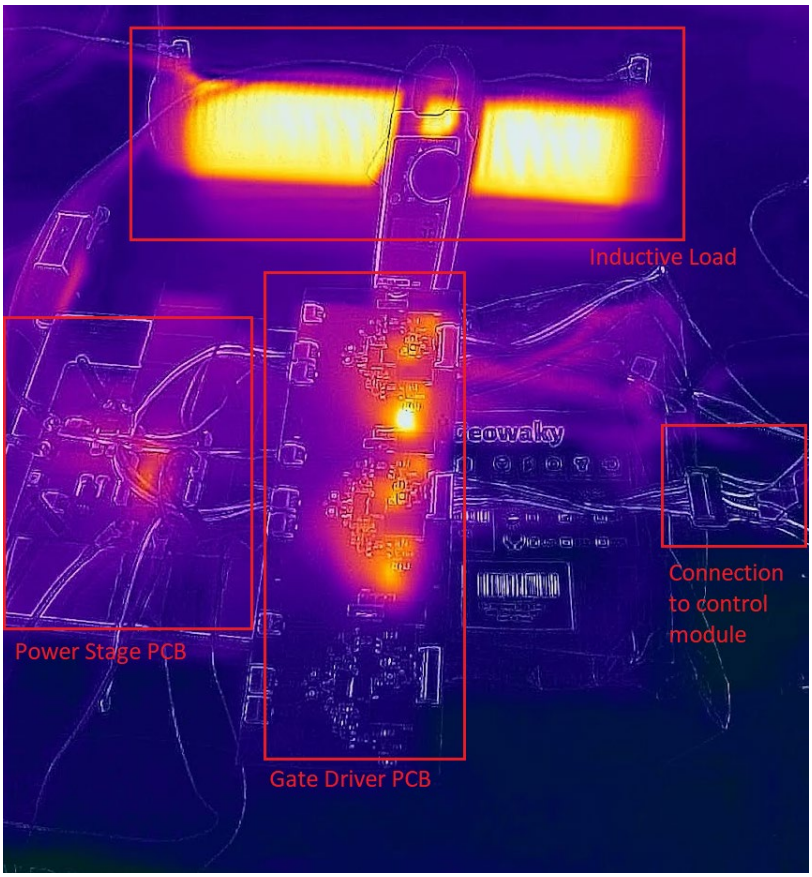

Figure 50: Thermal Image of system

Figure 51 shows the full test setup from the connection of the control module. The inductive load had a power rating of 1000W of 4.5 Ohms and 15 mH. Due to the options available for testing, loading the whole system under all three phases with a high voltage power supply was not possible, but tests showed that the system did function as intended. Only two current sensors were able to be sourced was admissible since the total of all three currents will sum to zero at any given time, meaning the third current can be calculated in the control board. Readings were also able to be recorded from the thermistor to provide the necessary information in the closed loop system and ensure the gate driver and SiC MOSFET were operating within their rated values. These results with the collaboration

with University of Augsburg were published in an article showing the findings of the tests and the potential of the SiC in the power electronics industry. [33]

The cost of the system will all parts considered ended up at $502.77. A bill of materials is included in Appendix C to show the breakdown of this cost. It should be noted that the cost of components will vary based on the amount ordered.

There are several improvements that could be made to the PCB for future versions that can be taken into consideration. Adding more ground planes to sections, specifically the output of the gate driver board could help reduce ringing and provide a cleaner signal on the input to the gates of the SiC MOSFETs. More temperature sensors could be added to provide more information to the system; this could take the form of adding SMD NTCs on the tops of the power traces on the DC input and AC output.

Chapter Five: Conclusion

5.1. Conclusion

Microgrids are becoming a larger and larger part in efforts of moving towards having a large percentage of the energy come from renewable sources in the US. Many houses and complexes will have RES of some kind with an ESS in conjunction. There are many different situations which impact design decisions on these inverters which are used in these systems. One of the goals of this thesis is to show the potential of SiC MOSFETs and wide band gap semiconductors as a viable candidate for these inverters. It also explores some of the control methods of grid forming and grid following and offers a simulation tool for these systems to aid in potential designs. There are areas that could be analyzed further and some parts in the testing that could have been taken further.

There are more facets of the microgrids that could be implemented into the simulations. Testing the inverter transitioning from grid connected to being islanded in case a fault on the grid could be simulated and tested. Other control schemes and other semiconductors could be researched in this system. Using SPICE models and implementing the thermal characteristics of the entire system with a heat sink would yield even more detailed results as well. More information from the real testing could have been found as well. During testing, while the three-phase system was validated under no load, sometime during setting up the system to be tested under load, one of the phases stopped working. This meant that

the test under load was only able test a single phase and not the whole system. Ideally this would have been fully functional. Conclusions can still be drawn from the data that was found and the system is viable for the system it was designed for, but more conclusive data is always preferred.

Microgrids and grid forming inverters will play a very large role in the future and SiC MOSFETs offer efficiencies that may offer competitive advantages in a market when homeowners or building owners are looking for adding a RES and ESS to their real estate. The goal of this thesis is to show SiC MOSFET's viability in this landscape and provide an investigation to simulate these systems in a power systems environment. The cost of the system with the displayed performance through the integration supports the claim that SiC MOSFETs are a competitive solution to high power inverters given the requirements of the system.

References

[1] Y. Zuo, Z. Yuan, F. Sossan, A. Zecchino, R. Cherkaoui and M. Paolone, "Performance assessment of grid-forming and grid-following converter-interfaced battery energy storage systems on frequency regulation in low-inertia power grids," *Sustainable Energy, Grids and Networks,* vol. 27, p. 100496, 2021.

[2] S. Anttila, J. Dohler, J. Oliveira and C. Boström, "Grid forming inverters: A review of the state of the art of key elements for Microgrid Operation," *Energies,* vol. 15, no. 15, p. 5517, 2022.

[3] Y. Lin, J. Eto, B. Johnson, J. Flicker, R. Lasseter, H. Pico, G.-S. Seo, B. Pierre and E. Abraham, "Research Roadmap on Grid-Forming Inverters," NREL, Golden, CO, 2020.

[4] Xcel Energy, "Net Energy Metering," Xcel Energy, 2021. [Online]. Available: https://co.my.xcelenergy.com/s/renewable/net-metering. [Accessed 22 2 2023].

[5] Ford Motor Company, "FORD INTELLIGENT BACKUP POWER," Ford Motor Company, 2022. [Online]. Available: https://www.ford.com/trucks/f150/f150-lightning/features/intelligent-backup-power/?intcmp=reVhp-featcta-intellBackup. [Accessed 22 2 2023].

[6] M. Laszlo, "Hummer EV Pickup Will Also Offer Power Station System," Hummer Nation, 2021. [Online]. Available: https://hummernation.com/2021/06/17/hummer-ev-pickup-will-also-offer-power-station-system/. [Accessed 22 2 2023].

[7] F. Groppi, "Testing of anti-islanding protections for grid-connected inverters," in *International Conference on Clean Electrical Power (ICCEP)* , Sicily , 2007.

[8] M. J. Ebrahimi, "General overview of maximum power point tracking methods for photovoltaic power generation systems," in *2015 30th International Power System Conference (PSC)*, Tehran, 2015.

[9] T. Rahman, "Low Noise Inverter for Poly Phase Microgrid System," in *International Conference on Computer and Communication Engineering (ICCCE)*, Kuala Lumpur, Malaysia, 2016.

[10] A. Kumar, M. Moradpour, M. Losito, W.-T. Franke, S. Ramasamy, R. Baccoli and G. Gatto, "Wide Band Gap Devices and Their Application in Power Electronics," *Energies,* vol. 15, no. 23, p. 9172, 2022.

[11] A. Yoshikawa, H. Matsunami and Y. Nanishi, Development and Applications of Wide Bandgap Semiconductors, 2007.

[12] F. Roccaforte, P. Fiorenza, G. Greco, R. L. Nigro, F. Giannazzo, F. Iucolano and M. Saggio, "Emerging trends in wide band gap semiconductors (SiC and GaN)," *Elsevier,* vol. 187, pp. 66-77, 2018.

[13] M. Beheshti, "Wide-bandgap semiconductors: Performance and Benefits of GaN versus SiC," *Analog Design Journal,* pp. 1-5, 2020.

[14] Typhoon HIL, "Three Phase Inverter," Typhoon HIL Documentation, 2022. [Online]. Available: https://www.typhoon-hil.com/documentation/typhoon-hil-software-manual/References/three-phase_two-level_inverter_rectifier.html. [Accessed 28 2 2023].

[15] L. Ibarra, P. Ponce and A. Molina, "An Adjustable Sensorless Shoot-Through Protection for H-Bridges," in *IECON 2018 - 44th Annual Conference of the IEEE Industrial Electronics Society*, Washington, DC, USA, 2018.

[16] I. Patrao, E. Figueres, F. González-Espín and G. Garcerá, "Transformerless topologies for grid-connected single-phase photovoltaic inverters," *Renewable and Sustainable Energy Reviews,* vol. 15, no. 7, pp. 3423-3431, 2011.

[17] K. Vasudevan, V. Ramachandaramurthy, T. Babu and A. Pouryekta, "Synchronverter: A Comprehensive Review of Modifications, Stability Assessment, Applications and Future Perspectives," *IEEE Access,* vol. 8, pp. 131565-131589, 2020.

[18] D. Pattabiraman, R. Lasseter and T. Jahns, "Comparison of Grid Following and Grid Forming Control for a High Inverter Penetration Power System," *2018 IEEE Power & Energy Society General Meeting,* pp. 1-5, 2018.

[19] O. Palizban, K. Kauhaniemi and J. Guerrero, "Microgrids in active network management—Part I: Hierarchical control, energy storage, virtual power

plants, and market participation," *Renewable and Sustainable Energy Reviews,* vol. 36, no. 1, pp. 428-439, 2014.

[20] Y. Han, H. Li, P. Shen, E. Coelho and J. Guerrero, "Review of Active and Reactive Power Sharing Strategies in Hierarchical Controlled Microgrids," *IEEE Transactions on Power Electronics,* vol. 32, no. 3, pp. 2427-2451, 2017.

[21] D. C. d. S, J. Dohler, P. Almeida and J. Oliveira, "Droop Control for Power Sharing and Voltage and Frequency Regulation in Parallel Distributed Generations on AC Microgrid," *IEEE International Conference on Industry Applications,* vol. 13, no. 1, pp. 1-6, 2018.

[22] F. Blaabjerg, "Reverse Droop Control-based Smooth Transfer Strategy for Interface Converters in Hybrid AC/DC Distribution Networks," *CSEE JOURNAL OF POWER AND ENERGY SYSTEMS,* vol. 9, no. 1, pp. 122-132, 2023.

[23] W. Sang, W. Guo, S. Wenyong , C. Tian, S. Yu and Y. Teng, "Virtual Synchronous Generator, a Comprehensive Overview," *Energies,* vol. 15, no. 1, p. 6148, 2022.

[24] A. Cherifi, A. Chouder, A. Kessal, A. Hadjkkadour, A. Aillane and K. Louassaa, "Control of Stand-Alone Inverter using Virtual Synchronous Generator," *2022 International Conference of Advanced Technology in Electronic and Electrical Engineering,* pp. 1-6, 2022.

[25] Q.-C. Zhong and G. Weiss, "Synchronverters: Inverters That Mimic Synchronous Generators," *IEEE TRANSACTIONS ON INDUSTRIAL ELECTRONICS,,* vol. 58, no. 4, pp. 1259-1267, 2011.

[26] K. M. Cheema, C. Naveed Ishtiaq, M. F. Tahir, K. Mehmood, M. Mudassir, M. Kamran, A. Milyani and Z. S. Elbarbary, "Virtual synchronous generator: Modifications, stability assessment," *Energy Reports,* vol. 8, pp. 1704-1717, 2022.

[27] B. Johnson, M. Rodriguez, M. Sinha and S. Dhople, "Comparison of Virtual Oscillator and Droop Control," in *NREL*, Stanford, California, 2017.

[28] H. Afshar, O. Husev, O. Matiushkin and D. Vinnikov, "A Review of Hybrid Converter Topologies," *Energies,* vol. 15, no. 1, p. 9341, 2022.

[29] Powersim, Inc, "Powering New Possibilities in Electronics Design," Powersim, Inc, 21 4 2023. [Online]. Available: https://powersimtech.com/. [Accessed 21 4 2023].

[30] A. Dunford, "3 Phase Gridlink Inverter with dq control design," PSIM, 10 8 2018. [Online]. Available: http://forums.powersimtech.com/t/gridlink-inverter-tutorial-video-circuit-file/327. [Accessed 15 4 2023].

[31] CREE, "C2M0280120D," 2 2021. [Online]. Available: https://assets.wolfspeed.com/uploads/2020/12/C2M0280120D.pdf. [Accessed 21 4 2023].

[32] Wolfspeed, "CCB021M12FM3 1200 V, 21 mΩ All-Silicon Carbide Six-Pack Module," 25 1 2021. [Online]. Available: https://assets.wolfspeed.com/uploads/2021/05/CCB021M12FM3.pdf. [Accessed 21 4 2023].

[33] C. Markgraf, L. Gacy S. Leitenmaier, D. Lengerer, B. Schwartz, and D. Gao, "Autonomous Electric Race Car Inverter Development," *IEEE Electrification,* pp. 1-12, 2023.

[34] WolfSpeed, "Wolfspeed WolfPACK™ Silicon Carbide Power Modules Family," WolfSpeed, 2021. [Online]. Available: https://www.wolfspeed.com/wolfspeed-wolfpack-sic-power-modules-family/#product-details. [Accessed 5 4 2023].

[35] F. Puhane, "DC Link Capacitor and Wireless Power Transfer," PSMA, 5 4 2020. [Online]. Available: https://www.psma.com/sites/default/files/uploads/files/DC%20Link%20Capacitor%20and%20Wireless%20Power%20Transfer%20A%20Perfect%20Couple%20Frank%20Puhane%20Wurth%20Electronics.pdf. [Accessed 2023 5 4].

[36] KEMET, "C4AU, Radial, 2 or 4 Leads, 500 - 1,200 VDC," 30 8 2021. [Online]. Available: https://www.mouser.com/datasheet/2/212/1/KEM_F3126_C4AU-2584772.pdf. [Accessed 6 4 2023].

[37] Texas Instruments, "UCC20520 4-A, 6-A, 5.7-kVRMS Isolated Dual-Channel Gate Driver with Single Input," 1 2022. [Online]. Available: https://www.ti.com/lit/ds/symlink/ucc20520.pdf?ts=1673192830492. [Accessed 6 4 2023].

[38] RECOM, "RSOE(-Z) RECOM DC/DC Converter," 4 2020. [Online]. Available: https://www.mouser.com/datasheet/2/468/RSOE-1948033.pdf. [Accessed 6 4 2023].

[39] Analog, "Slew Rate Controlled Ultralow Noise 1A Isolated DC/DC Transformer Driver," 5 2 2003. [Online]. Available: https://www.analog.com/en/products/lt3439.html#product-overview. [Accessed 6 4 2023].

[40] Allegro, "ACS770xCB: Thermally Enhanced, Fully Integrated, Hall Effect-Based High Precision Linear Current Sensor IC with 100 μΩ Current Conductor," 12 10 2021. [Online]. Available: https://www.allegromicro.com/en/products/sense/current-sensor-ics/fifty-to-two-hundred-amp-integrated-conductor-sensor-ics/acs770. [Accessed 6 4 2023].

[41] KiCAd, "KiCad EDA A Cross Platform and Open Source Electronics Design Automation Suite," KiCad, 25 12 2021. [Online]. Available: https://www.kicad.org/. [Accessed 6 4 2023].

[42] N. Mohammed, M. Ali, M. Ciobotaru and J. Fletcher, "Accurate control of virtual oscillator-controlled islanded AC microgrids," *Electric Power Systems Research,* vol. 214, p. 108791, 2023.

[43] D. B. Rathnayake, M. Akrami, C. Phurailatpam, S. P. Me, S. Hadavi, G. Jayasinghe, S. Zabihi and B. Bahrani, "Grid Forming Inverter Modeling, Control, and Applications," *IEEE Access,* vol. 9, no. 1, pp. pp. 114781-114807, 2021.

Appendix A

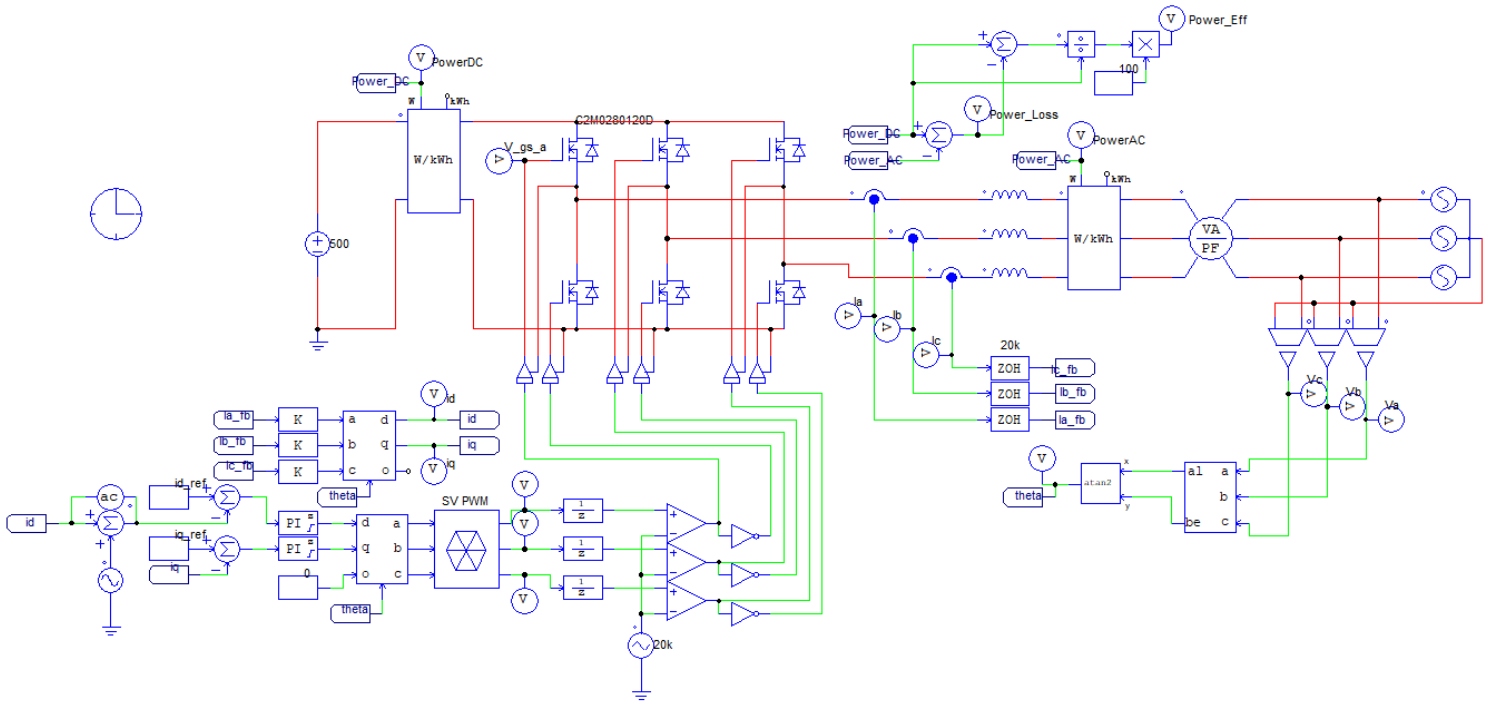

3phase_gridlink_nonideal_MOSFET_grid following.psimsch

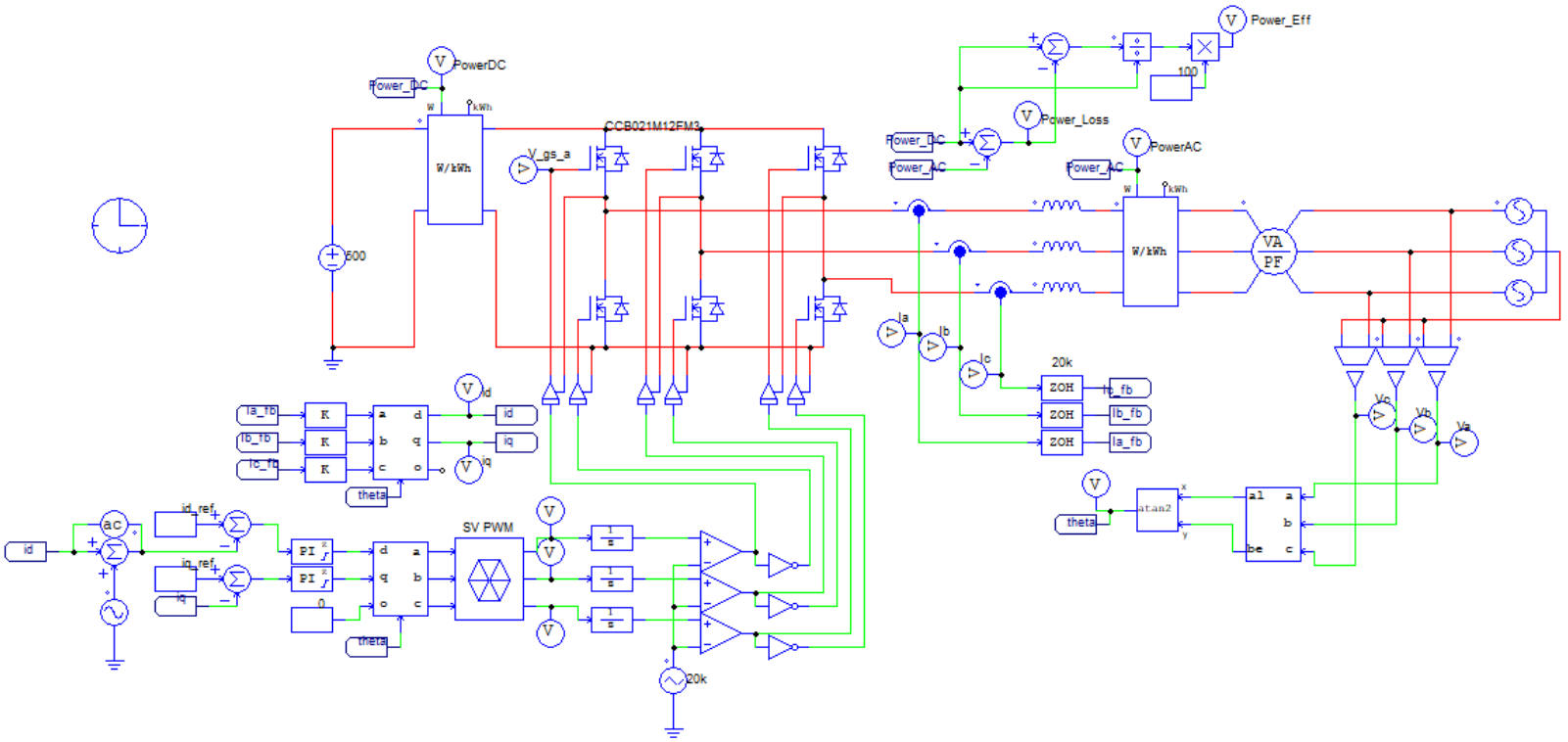

3phase_gridlink_nonideal_MOSFET_grid following_Wolf_speed_MOSFET.psimsch

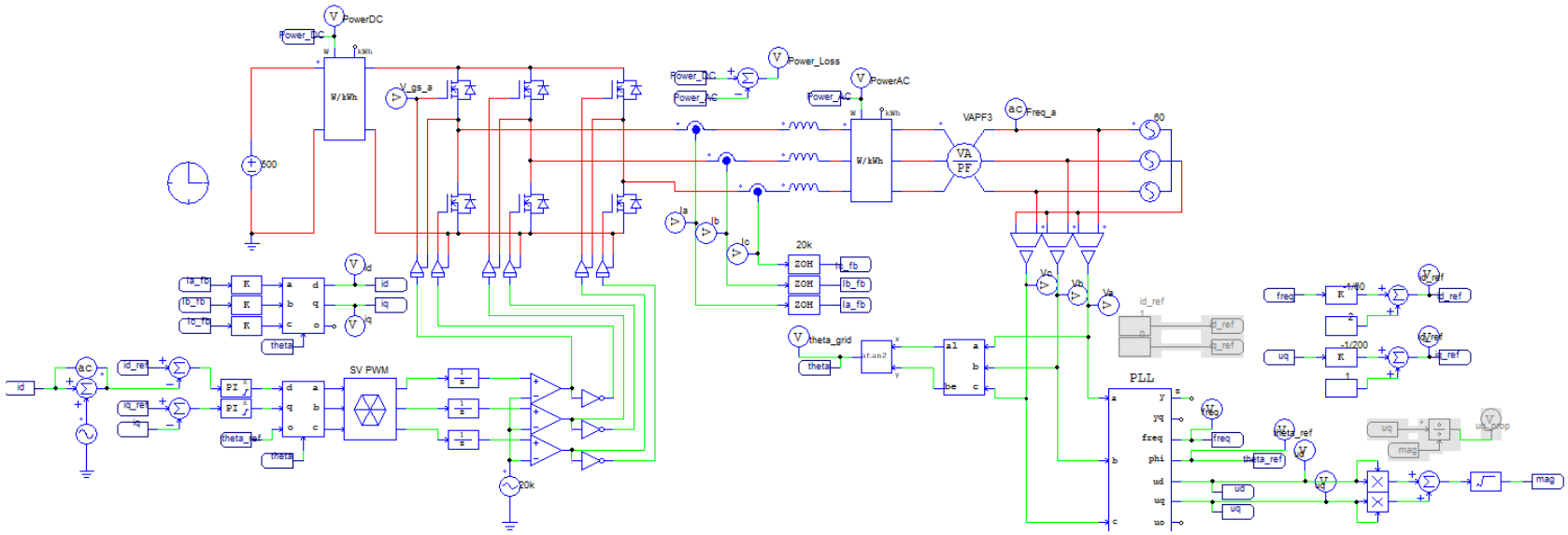

3phase_gridlink_nonideal_MOSFET_grid_forming_r_droop.psimsch

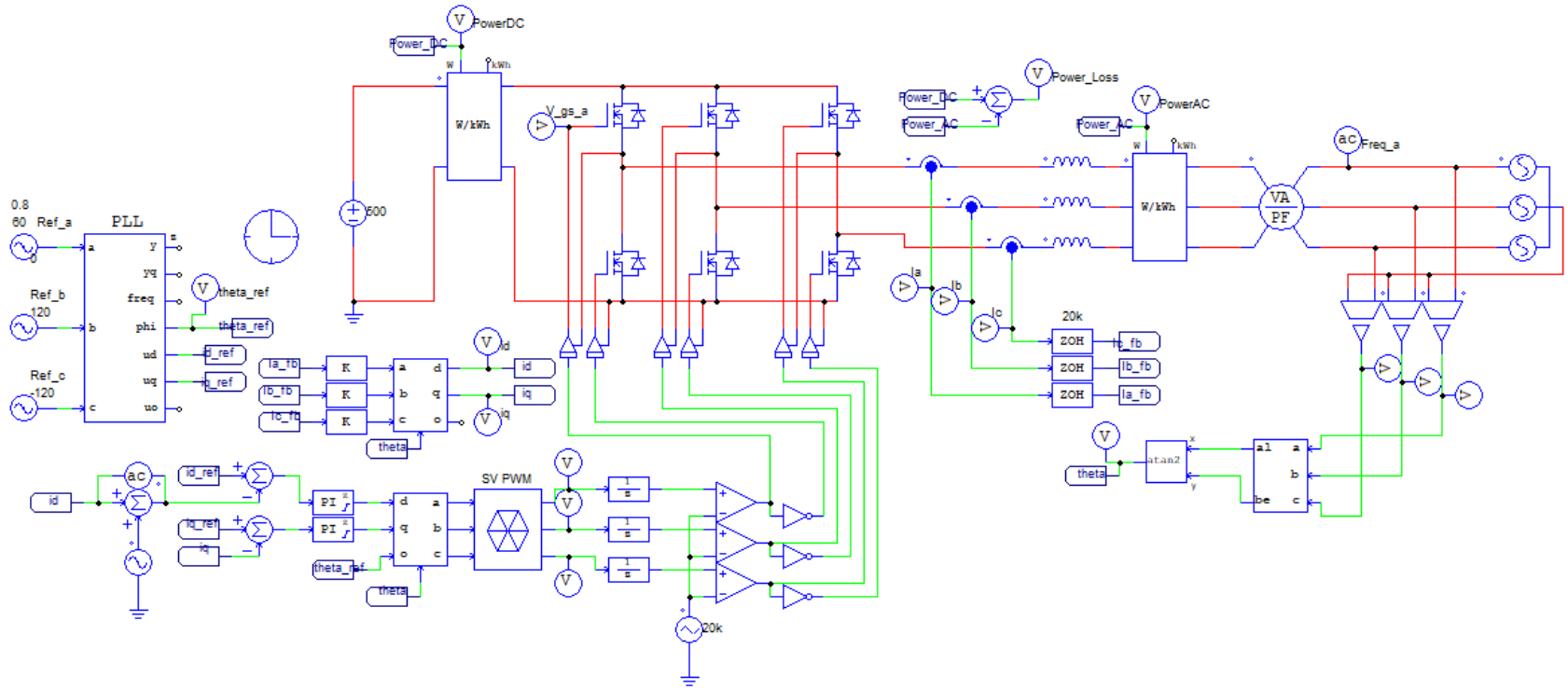

3phase_gridlink_nonideal_MOSFET_grid_forming_VSG.psimsch

Appendix B

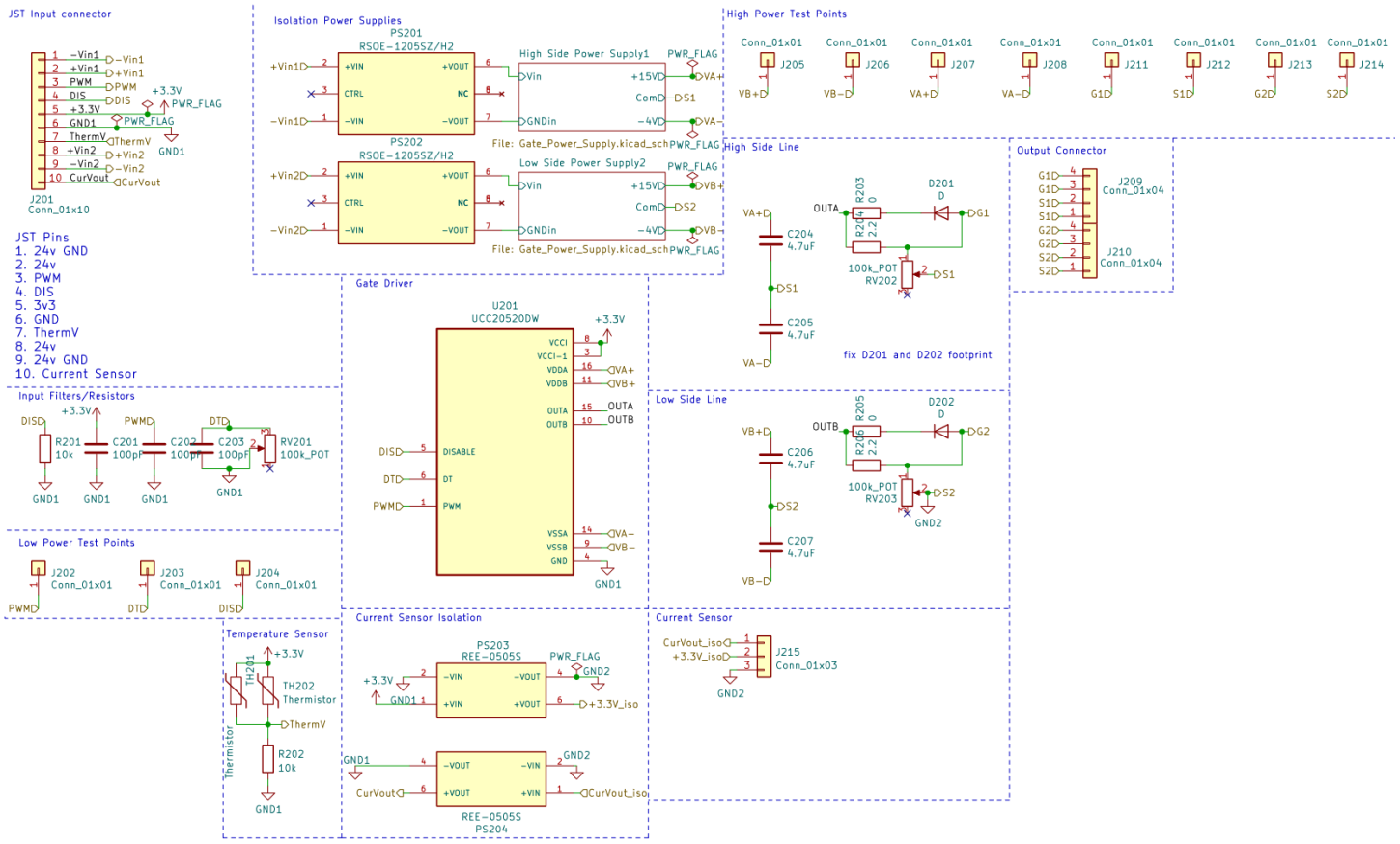

Schematic of single phase of gate driver board

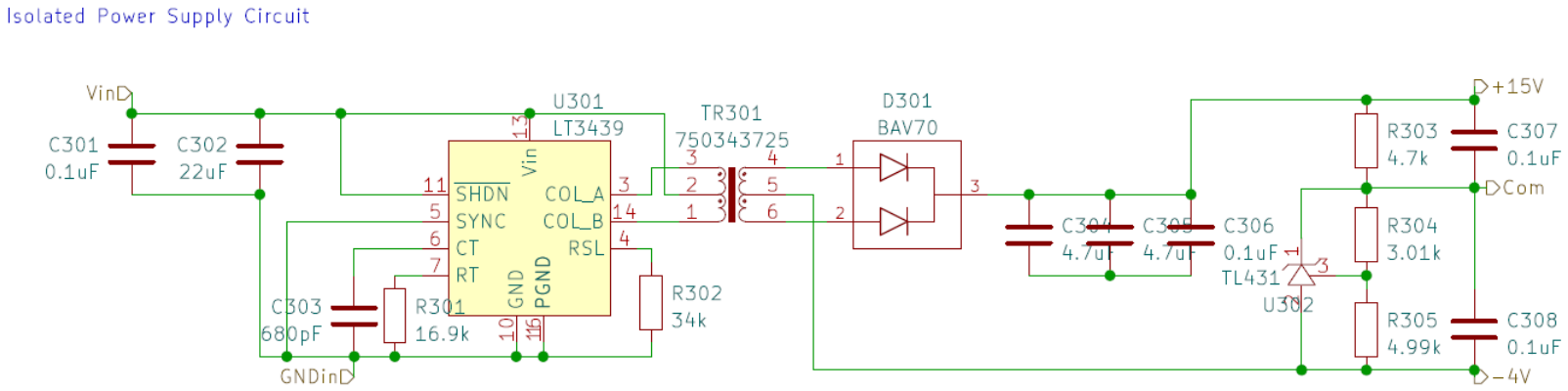

Isolated power supply circuit (Same for high and low side) subcircuit

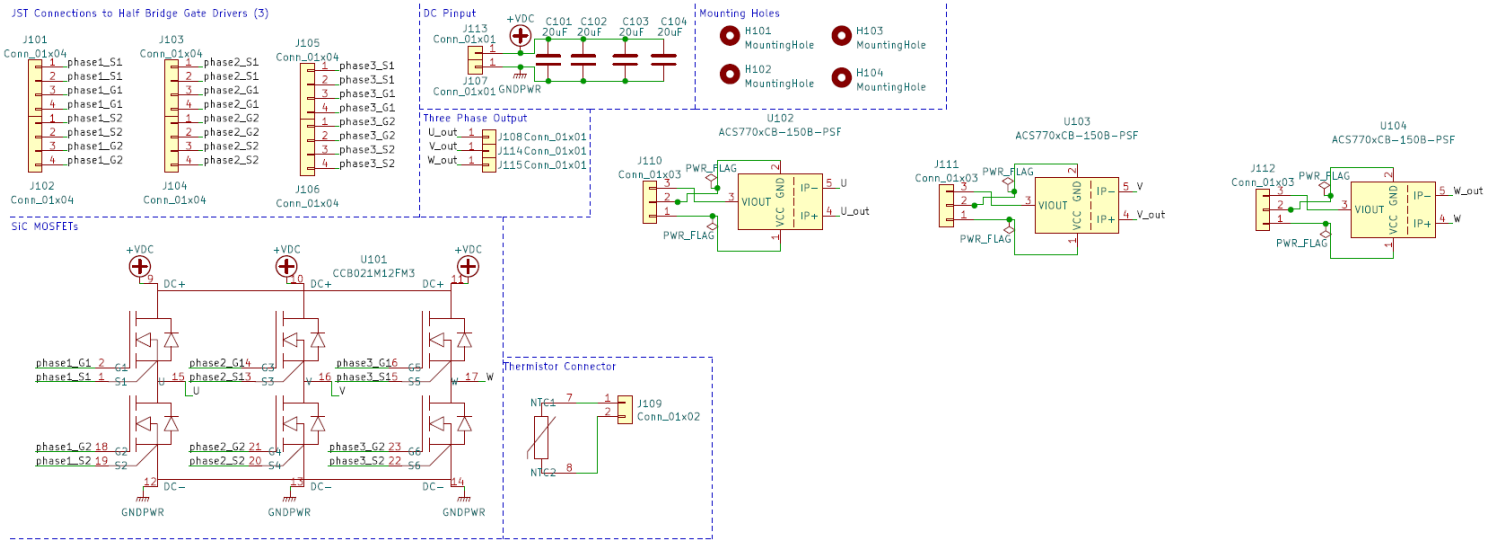

Power Stage Module Schematic

Appendix C

Bill of Materials					
Gate Driver					
Item	Qty	Reference(s)	Value	Price per unit	Total Price
1	9	C201, C202, C203, C501, C502, C503, C801, C802, C803	100pF	$0.10	$0.90
2	24	C204, C205, C206, C207, C304, C305, C404, C405, C504, C505, C506, C507, C604, C605, C704, C705, C804, C805, C806, C807, C904, C905, C1004, C1005	4.7uF	$0.10	$2.40
3	24	C301, C306, C307, C308, C401, C406, C407, C408, C601, C606, C607, C608, C701, C706, C707, C708, C901, C906, C907, C908, C1001, C1006, C1007, C1008	0.1uF	$0.10	$2.40
4	6	C302, C402, C602, C702, C902, C1002	22uF	$0.10	$0.60
5	6	C303, C403, C603, C703, C903, C1003	680pF	$0.10	$0.60
6	6	D201, D202, D501, D502, D801, D802	D	$0.63	$3.78
7	6	D301, D401, D601, D701, D901, D1001	BAV70	$0.08	$0.48
8	3	J201, J501, J801	Conn_01x10	$0.10	$0.30
9	6	J209, J210, J509, J510, J809, J810	Conn_01x04	$0.10	$0.60
10	3	J215, J515, J815	Conn_01x03	$0.10	$0.30
11	6	PS201, PS202, PS501, PS502, PS801, PS802	RSOE-2405SZ/H2	$10.05	$60.30
12	3	PS203, PS503, PS803	REE-0505S	$3.33	$9.99
13	3	PS204, PS504, PS804	REE-0505S	$3.33	$9.99
14	6	R201, R202, R501, R502, R801, R802	10k	$0.10	$0.60
15	6	R203, R205, R503, R505, R803, R805	0	$0.10	$0.60
16	6	R204, R206, R504, R506, R804, R806	2.2	$0.10	$0.60
17	6	R301, R401, R601, R701, R901, R1001	16.9k	$0.10	$0.60
18	6	R302, R402, R602, R702, R902, R1002	34k	$0.10	$0.60

19	6	R303, R403, R603, R703, R903, R1003	4.7k	$0.10	$0.60
20	6	R304, R404, R604, R704, R904, R1004	3.01k	$0.10	$0.60
21	6	R305, R405, R605, R705, R905, R1005	4.99k	$0.10	$0.60
22	9	RV201, RV202, RV203, RV501, RV502, RV503, RV801, RV802, RV803	100k_POT	$0.64	$5.76
23	3	TH201, TH501, TH801	Thermistor	$0.49	$1.47
24	3	TH202, TH502, TH802	Thermistor	-	0
25	6	TR301, TR401, TR601, TR701, TR901, TR1001	750343725:	$7.13	$42.78
26	3	U201, U501, U801	UCC20520DW	$6	$18
27	6	U301, U401, U601, U701, U901, U1001	LT3439	$9.54	$57.24
28	6	U302, U402, U602, U702, U902, U1002	TL431	$0.53	$3.18
30	1	PCB		$16.80	$16.80
Power Stage					
Item	Qty	Reference(s)	Value		
1	4	C101, C102, C103, C104	20uF	$6.97	$27.88
2	6	J101, J102, J103, J104, J105, J106	Conn_01x04	$0.10	$0.60
3	2	J107, J113	Conn_01x01	$0.10	$0.20
4	3	J108, J114, J115	Conn_01x01	$0.10	$0.30
5	1	J109	Conn_01x02	$0.10	$0.10
6	3	J110, J111, J112	Conn_01x03	$0.10	$0.30
7	1	U101	CCB021M12FM3	$169.23	$169.23
8	3	U102, U103, U104	ACS770xCB-150B-PSF	$4.33	$12.99
9	1	PCB		$48.50	$48.50
		Price will vary based on quantity ordered		Total Price	$502.77